REVIEW

Check for updates

Exploring the efficacy and future potential of polypyrrole/metal oxide nanocomposites for electromagnetic interference shielding: a review

Yuvika Sood, [iD] [a] Harish Mudila, [iD] [a] Pankaj Chamoli, [iD] [b] Parveen Saini [iD] *[c] and Anil Kumar [iD] *[a]

With recent advancements in technology, the emission of electromagnetic radiation has emerged as a significant issue due to electromagnetic interferences. These interferences include various undesirable emissions that can degrade the performance of equipment and structures. If left unresolved, these complications can create extra damage to the security operations and communication systems of numerous electronic devices. Various studies have been conducted to address these issues. In recent years, electrically conductive polypyrrole has gained a unique position because of its many advantageous properties. The absorption of microwaves and the electromagnetic interference (EMI) shielding characteristics of electrically conductive polypyrrole can be described in relation to its great electrical conductivity with strong relaxation and polarization effects due to the existence of strong bonds or localized charges. In the present review, advancements in electromagnetic interference shielding with conjugated polypyrrole and its nanocomposites with metal oxides are discussed and correlated with various properties such as dielectric properties, magnetic properties, electrical conductivity, and microwave adsorption properties. This review also focuses on identifying the most suitable polypyrrole-based metal oxide nanocomposites for electromagnetic interference shielding applications.

Wider impact

We report in this review the recent advances in polypyrrole/metal oxides nanocomposites for electromagnetic interference (EMI) shielding applications. The effect of different fillers in the matrix of polypyrrole and their impact on the shielding performance are summarized in the manuscript. This area of study shows significant wider interest as co-relations have been built between the structure–properties–applications of polymeric materials for ensuring effective shielding performance. This review may be especially beneficial for researchers working in the field of the processability of conjugated polymeric materials and the tuning of the structure for effective EMI shielding performance. It should make it easier for them to select specific materials for EMI shielding with different structures correlated with different properties. Substantial improvements in the structural, mechanical, electrical, and thermal properties of polypyrrole/metal oxides nanocomposites are required for effective EMI shielding performance over metal-based EMI shields.

1. Introduction

The increasing prevalence of diverse electrical products and technology has resulted in an increase in electromagnetic pollution to very high levels in the environment. In recent times, the escalation of this electromagnetic (EM) pollution is attributable to the rapid advancements in modern communication technology.[1–3] The occurrence of electromagnetic radiation interference in the high-frequency radio frequency (RF) and microwave bands can have detrimental effects on the human body, including an increased risk of cancer, anxiety, asthma, heart diseases, migraine, sleep disruption, and even miscarriage with prolonged exposure. Recognizing the significant threat posed by electromagnetic interference (EMI), it has become imperative to effectively reduce such radiation.[4] The practice of mitigating EM radiation through the use of barriers made from conducting or magnetic materials is referred to as EMI shielding.[5,6] EMI shielding is important because it helps to maintain the integrity of signals within electronic circuits,

[a] Department of Chemistry, Lovely Professional University, Phagwara, Punjab, 144411, India. E-mail: rsanil.nit@gmail.com

[b] Department of Physics, Shri Guru Ram Rai University, Dehradun, Uttarakhand, 248001, India

[c] Conjugated Polymers, Graphene Technology and Waste Management Lab, Advance Materials and Devices Metrology Division, CSIR-National Physical Laboratory, Delhi-110012, India. E-mail: pksaini@nplindia.org

preventing data errors and ensuring reliable communication between components. It also prevents brownouts, blackouts and sudden power fluctuations. To meet the EMI challenges, there has been a rapid and extensive development and utilization of electromagnetic wave-absorbing materials in both military and commercial applications over the past few decades.[7,8] Materials with a broad frequency bandwidth, minimal thickness, lightweight design, and robust absorption capabilities have consistently been the focal point in the pursuit of effective EM wave absorbers and effective EMI shields to ensure the optimal functioning of electro/electrical systems.[9] Materials with such properties can serve as a protective barrier for shielding electronic devices from undesired electromagnetic

radiations. Similar to a protective coating, EMI shields play a crucial role in managing electromagnetic interference from both incoming and outgoing waves.[10] An established approach to address EMI involves the strategic utilization of lossy dielectric and magnetic materials, which can effectively shield electronic devices through the absorption and reflection of unwanted electromagnetic radiation.[11–13] Typically, shielding materials with dominant absorption properties are more suitable for devices, as relying on reflection may potentially aggravate interference effects on nearby devices.[14] Earlier, metals and their composites were used as EMI shielding materials. Such materials have shown high EMI shielding effectiveness on account of their better high electrical

Yuvika Sood

Yuvika Sood is currently a research scholar and PhD student in the Department of Chemistry at Lovely Professional University, Jalandhar. She is working in the area of conductive polymer nanocomposites for gas sensing. She completed her bachelor's degree at Chaudhary Sarwan Kumar Himachal Pradesh Vishvavidyalaya, Palampur (India) and received her master's degree in Chemistry from Shoolini University, Solan. Currently her research interests include the synthesis of different nanostructures of metal sulfides and their application in gas sensors.

Harish Mudila

Dr Harish Mudila is an Associate Professor in the Department of Chemistry at Lovely Professional University, Punjab. He obtained his PhD from G. B. Pant University of Agriculture & Technology, Pantnagar. Uttarakhand, in the field of electrochemical energy storage, gas sensing, and soft materials.

Pankaj Chamoli

Dr Pankaj Chamoli is an associate professor in the Department of Physics at Sri Guru Ram Rai University, Dehradun, Uttarakhand, India. He earned his PhD in Materials Science from the Materials Science Programme at IIT Kanpur, Uttar Pradesh, India. He also holds an MTech in Materials & Metallurgical Engineering from Thapar University, Patiala, Punjab, as well as undergraduate and postgraduate degrees in Physics from HNB Garhwal University, Srinagar, Uttarakhand. His work spans various areas of nanoscience and technology, with a particular focus on nanostructured materials, carbon nanomaterials (such as graphene), nanocomposites, nanocolloids, soft materials, and their applications in EMI shielding, microwave absorption, water purification, photocatalytic activity, energy storage/conversion, and various biological applications.

Parveen Saini

Dr Parveen Saini joined CSIR-National Physical Laboratory (CSIR-NPL), New Delhi, India, 19-years ago as a Jr. Scientist, and is now working as Sr. Principal Scientist. He received his Bachelor of Engineering Degree in Polymer Science and Chemical Technology from Prestigious Delhi College of Engineering (DCE now DTU), New Delhi, in 2002 and PhD (part-time) in Conducting Polymers from Centre for Polymers Science and Engineering (CPSE), Indian Institute of Technology Delhi (IITD), in 2012. His research interests include conducting polymers, carbon nanotubes, graphene and their nanocomposites, polymer technology and waste to wealth strategies for applications in areas including but not limited to electromagnetic interference (EMI) shielding, water purification, anticorrosion & self-cleaning coatings, sensors/detectors, battery/supercapacitors, etc.

conductivity, mechanical properties, and good permeability.[15] The efficacy of metals in shielding is attributed to their enhanced reflection mechanism.[16] However, these materials also have some significant drawbacks such as limited mechanical flexibility, lack of processability, high density, and susceptibility to corrosion.[17] Over the last two decades, researchers have redirected their focus towards conducting polymeric materials such as polyaniline (PANI), polypyrrole (PPy), poly(3,4-ethylenedioxythiophene):polystyrenesulfonate (PEDOT:PSS), polyvinylidene fluoride (PVDF), and polythiophene (PTP).[18,19]

Among these conducting polymers, PPy has a unique position for EMI shielding due to its good electrical conductivity, good environment stability, facile synthesis, and good corrosive resistance.[20] However, PPy is infusible, insoluble, and has poor mechanical strength and poor processibility, which have limited its commercialization.[21] To solve these limitations of PPy, constituent materials have been combined in matrices to create materials with different physical and chemical properties, also known as composites.[22,23] There are various types of composites, like metal matrix composites (MMCs), ceramic matrix composites (CMCs), and polymer–matrix composites (PMCs). PMCs in comparison with MMCs and CMCs have great importance due to their ease of production, low cost, light weight, and relatively low processing temperatures (at high temperature, polymers begin to degrade), forming the foundation for a vast range of applications in various industries worldwide. The tailored formation of these composites can tune various properties, like structural, electrical, thermal, mechanical, magnetic, dielectric, and microwave-absorption properties.[24] The evaluations of such kinds of properties in composites involve consideration of the dispersible interface of the matrix and filler materials. However, the development of good quality composites depends on various parameters, like the selection of the matrix, filler, solvent, temperature, and user carefulness during

Dr Anil Kumar is currently working as an assistant professor of Chemistry at Lovely Professional University, Jalandhar Punjab. He completed his PhD at the Malaviya National Institute of Technology (MNIT) Jaipur, India in the area of conducting polymer nanocomposites. Dr Kumar also holds an MTech in Materials & Metallurgical Engineering from Thapar University, Patiala, Punjab, India. He completed his BSc (Non-Medical) and MSc (Chemistry) at Himachal Pradesh University, Shimla and Panjab University, Chandigarh, respectively. His foremost areas of research expertise are in materials chemistry, conducting polymer nanocomposites for EMI shielding, Gas sensing and optoelectronic devices.

Anil Kumar

processability. During the formation of a dispersible interface with the matrix and fillers, each component loses their own identity and evolves the desired identity that is required for the particular application. Polypyrrole's limited mechanical strength and processability hinder its applicability in commercial settings.[25,26] In such instances, utilizing conducting polymer composites with well-suited fillers is an excellent alternative strategy, allowing for the creation of a tunable shield at microwave frequencies.[27] Enhancing the electromagnetic (EM) absorption performance of PPy can be approached in two ways. First, by focusing on refining the morphology and structure of pure PPy, and second, by fabricating composites in which the single dielectric-loss material PPy is elaborately hybridized with other dielectric-loss materials (primarily comprising graphene,[28,29] carbon nanotubes,[30,31] and other conductive polymers)[32,33] and magnetic materials (such as ferrite, metals, metal oxides,[34,35] and Mxenes[36]). Among these, metal oxides are considered especially good for EMI shielding due to their strong reflective properties and high electrical conductivity. It is well known that the presence of oxygen widely affects the electrical, magnetic, and shielding performances of a material. Jones *et al.* reported the stoichiometric effect of oxygen on the electrical properties of chromium oxide (Cr_2O_3), niobium pentoxide (Nb_2O_5), ceric oxide (CeO_2), thorium oxide (ThO_2), and gallium oxide (Ga_2O_3). They reported that the conductivities of Cr_2O_3, Nb_2O_5, and CeO displayed a switch-like behavior under a stoichiometric mixture of oxygen and a reducing gas, whereas Ga_2O_3 and ThO_2 did not exhibit this type of behavior. Due to the p-type semiconducting nature of chromium oxides, the increasing concentration of oxygen (with N_2 + CO) resulted in increasing conductivity. In the case of niobium pentoxides and ceric oxide, both showed an n-type behavior and their conductance dropped with increasing the oxygen concentration (with N_2 + CO). The p-type behavior of thorium oxide showed an increase in conductance with increasing oxygen concentration (with N_2 + CO). The regular increment in conductance was not seen at a stoichiometric ratio.[37] Zang *et al.* reported using first-principles calculations that the magnetic properties of metal oxides depend on the magnetic moment of the oxygen atom. They explained that magnetic properties of antiferromagnetic oxide (Ba_2CoO_4) are dominated by the moment of the oxygen atom, and that this is the reason for the occurrence of a magneto-elastic response and long-range magnetic ordering.[38]

The extended use of these materials is hindered by issues like corrosion and their vulnerability leading to intermodulation problems, as well as their heavy weight, which compromises their physical and mechanical stability over time. The various properties correlated with EMI shielding are magnetic, dielectric, and microwave electromagnetic absorption, and these are extensively described in the present article. Luo *et al.* synthesized PPy/Co nanocomposites, which was confirmed using different characterizations, for EMI shielding.[39] The results showed that the PPy/Co nanocomposites exhibited superior absorption performance compared to their individual components, suggesting their

potential in microwave absorption. With the increase in the matching thickness, the absorption peaks varied toward the low-frequency direction. When the matching thickness was 3.0 mm, the value of the maximum R_L was -20.0 dB at 13.8 GHz with a 7.2 GHz bandwidth. Olad *et al.* reported that the maximum reflection loss reached -32.53 dB at 9.95 GHz with a thickness of 2 mm for an epoxy-PPy/Fe$_3$O$_4$–ZnO quaternary NC when the Fe$_3$O$_4$/ZnO ratio was $1:2$.[40]

Vineeta Shukla reported that metals with various oxides show good shielding performance by means of both absorption and reflection processes. The porous structure of metal oxides can improve the shielding performance due to their good surface area, complimentary permeability, low density, and disciplinable internal structure. These properties enhance the multiple reflections of radiation in the porous structure of metal oxides.[41]

A wide absorption area and high attenuation may be responsible for the dielectric loss of PPy, magnetic loss factor of Fe$_3$O$_4$, and their synergetic effects. A closer look at Fig. 1 reveals the rapid progress on the research into PPy-based nanocomposites for EMI shielding based on the increasing research and review articles in this field in the last decade. A year by year breakdown of the data reveals a marked increase in the research activity leading up to 2023. This increase can be linked to the growing intrigue and technological progress surrounding PPy-based nanocomposites, especially given their crucial role in EMI shielding.

Herein, we review the recent advances in PPy-based composites using metal oxides for EMI shielding. The effect of different fillers in the matrix of PPy and their impact on the shielding performance are summarized. To the best of our knowledge, the shielding performance of PPy-based composites using the above-mentioned filler has not been reported till now. In addition to this, we report on the co-relations between the properties of polymeric materials that are required for effective shielding performance.
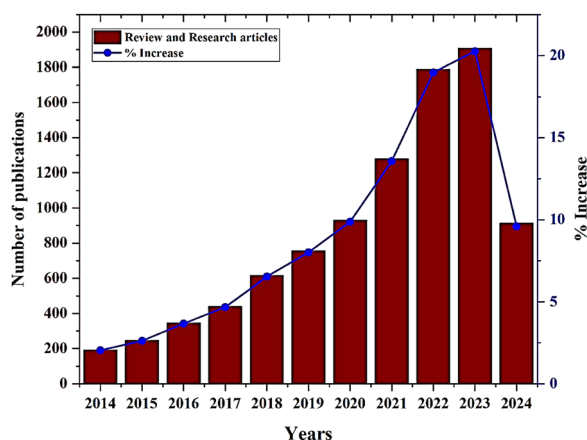

Fig. 1 Research publications based on PPy-based nanocomposites for EMI shielding in the last decade.

2. Basic mechanism of EMI shielding

Shielding efficiency, which is defined as the ratio of incident EM waves striking a material without shielding to the EM waves with the shielding material, is the main measure indicating the shielding effectiveness caused by the attenuation of electromagnetic energy. Permittivity, permeability, and electrical conductivity are thought to be the main causes of microwave attenuation in accordance with electromagnetic interference (EMI) theory.[42] EMI-SE is expressed as:

$$\text{Shielding efficiency (SE)} = \text{magnitude of incident}$$
$$\text{EM waves without shielding/magnitude of incident}$$
$$\text{EM waves with shielding} \qquad (1)$$

Based on the SE and EMI, the electromagnetic interference (EMI) shielding response can be measured. Three alternative techniques, involving the reflection, absorption, and multiple reflections of EM waves, can be used to create a shield. The sum of the reflection, absorption, and multiple internal reflections is known as the total shielding efficiency (SE), and is calculated by eqn (2). These processes are responsible for electromagnetic energy. The mechanism responsible for electromagnetic energy attenuation is presented in Fig. 2.

$$\text{SE}_\text{T} = \text{SE}_\text{R} + \text{SE}_\text{A} + \text{SE}_\text{M} \qquad (2)$$

The usage of polymer nanocomposites can improve the electrical conductivity of conducting nanofillers and their ability to connect networks, and create magnetic and electrical field dipoles for EMI shielding.

Shielding by reflection (SE$_\text{R}$) occurs whenever electromagnetic radiation strikes a shielding material that contains active charge carriers, because the reflected radiation interacts with the electrons and holes in the substance. Due to the mismatch in impedance between the incoming electromagnetic signals and the shielding nanomaterial, the microwave region experiences a reflection of waves. Metals are commonly thought to have superior conductivity, and the main process by which they attenuate electromagnetic energy is reflection.[43] The extent of the reflected rays can be calculated by eqn (3).

$$\text{SE}_\text{r} = -10 \log_{10}\left(\frac{\sigma T}{16\omega\varepsilon_0 u_r}\right) \qquad (3)$$

Shielding by absorption (SE$_\text{A}$) creates shielding to absorb incident electromagnetic waves as the second step in the shielding procedure.[44] It is anticipated that materials having active electric and/or magnetic dipoles may attenuate the EM energy by an absorption process. Materials used as shielding for the adsorption of EM waves require the dipoles of electric and magnetic fields. Within the thickness of the shielding materials, the EM wave-propagation range progressively decreases. The absorption is mainly caused by Ohmic current created in the shield and by magnetic hysteresis losses.[13] Eqn (4) below can be used to calculate the amount of shielding by absorption.

$$\text{SE}_\text{A} = -8 \times 68t\left[\frac{\sigma_T \omega u_\gamma}{2}\right]1/2 \qquad (4)$$
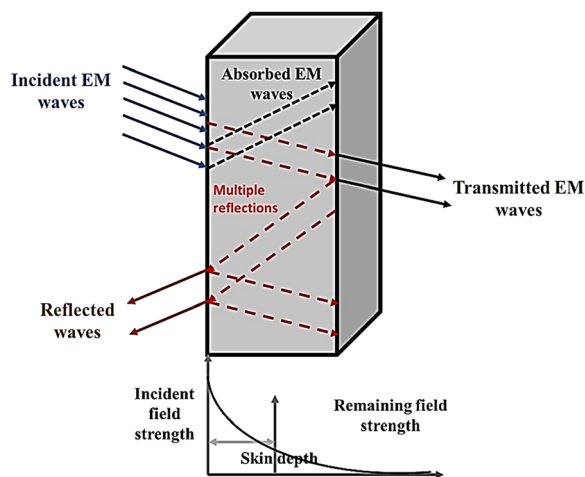
Fig. 2 Basics mechanism of EMI shielding.

Shielding effectiveness through multiple reflections (SE$_{MR}$) is based on multiple total internal reflections adding a shielding effect in materials with layered structures and changed interfaces. Due to the fact that the action occurs inside the barrier, this technique can aid in improving absorption. When the absorption contribution is greater, the numerous reflections are very modest in intensity and can be disregarded. Typically, only shielding surfaces that are electrically conductive are used to include extreme frequency radiation, and even then, only to the extent that doing so exponentially reduces the field by thickening the surface. This can be calculated using the following equation.

$$\delta = \frac{1}{\sqrt{\Pi f u \sigma}} \qquad (5)$$

When the shielding thickness is minimal relative to the skin effect, the EM radiation is reflected at many borders within the shielding nanomaterials. Various techniques can be employed to determine the degree of shielding caused by multiple reflections using eqn (6).

$$SE_{MR} = 20 \log_{10}\left(1 - e^{-2t/\delta}\right) \qquad (6)$$

The effectiveness of multiple reflection shielding is closely related to the absorption capacity protecting nanomaterials. It is clear from the equation that the thickness and high absorbance (SE$_A$) of the shield are more prominent aspects and one can easily ignore the value of SE$_{MR}$. The main reason is that at the maximum frequency, even though the EM radiation moves from one surface edge to another, the range of electromagnetic radiation becomes negligible due to absorption.[45]

3. Polypyrrole/metal oxide nanocomposites for EMI shielding

Recognized for their outstanding electrical conductivity and permeability, metallic materials, such as silver, copper, iron, and nickel, are recognized as crucial components for electromagnetic interference (EMI) shielding in electronic devices. However, their widespread use in EMI shielding applications is hindered by certain inherent drawbacks, including high density, vulnerability to corrosion, and limited flexibility, which pose significant challenges for their application. To overcome the disadvantage of traditional metal-type shielding materials, such as their rigidity and high density, metal/polymer composites are a good choice, which combine the excellent conductivity of metals with the outstanding mechanical properties of polymers.

Magnetic nanocomposites were prepared by Azadmanjiri *et al.* using an *in situ* oxidative polymerization technique to envelop varying quantities of iron oxide nanoparticles (MNPs) within the conductive polymer polypyrrole (PPy). These nanocomposites were subsequently blended into an epoxy resin matrix at different weight fractions, including 10, 20, and 30 wt%. The DC conductivity was reduced for higher weight fractions of insulating MNPs, whereas the saturation magnetization (σ_s) increased. This decrease could be attributed to a reduction in the conductive pathways in PPy due to the embedded MNPs. Also, the higher content of MNPs in the composite particles naturally led to higher values of σ_s. Nanocomposites were developed by incorporating MNP/PPy composite nanoparticles, where both the magnetic and conducting components coexisted in close contact. The EMI shielding behavior was assessed using a vector network analyzer in the frequency range of 0.1–18 GHz. Notably, they exhibited a significant improvement in absorption, reaching 10.10 dB at the upper limit of the frequency range (17–18 GHz) of the instrument. This enhancement was compared to the absorption capabilities of individual PPy particles (7.5 dB), individual MNPs (2.6 dB), or physical mixtures of MNPs and PPy particles (3.6 dB) within the resin. The results demonstrated that the samples containing 10 wt% (PPy/30% MNP) composite nanoparticles showed enhanced absorption properties in comparison with the samples prepared by directly blending PPy with MNPs in epoxy resin with the same ratio or either of the components alone in the epoxy. It is proposed here that this improvement may result from a better match between the dielectric loss, magnetic loss, and an improved dispersion of the magnetic/conductive nanocomposites in the matrix.[21]

Ebrahimi and co-workers reported the shielding efficiency due to reflection (SE$_R$) and the total shielding efficiency SE$_T$ (EMI-SE) of the samples in the C-band frequency range of 4.7–7.7 GHz. The results are shown in Fig. 3. They observed that MWCNTs interaction with electromagnetic waves resulted in reflections due to the mobile carriers, while conductive paths could also increase the reflections. The observed variation of electromagnetic reflections for COOH-MWCNT was between 6.2 dB to 18 dB in the 4–8 GHz frequency range. The incorporated PPy increased the reflection of EM waves because of the enhanced conductive network in the PPy-MWCNT composite with a modified phase boundary and charge carriers. From Fig. 3(a), it could be observed that SE$_R$ varied from 1 dB to 33 dB, with a sharp peak at 7.45 GHz. The PPy-MWCNT–Ag samples showed a reflection at ∼24 dB with the disappearance
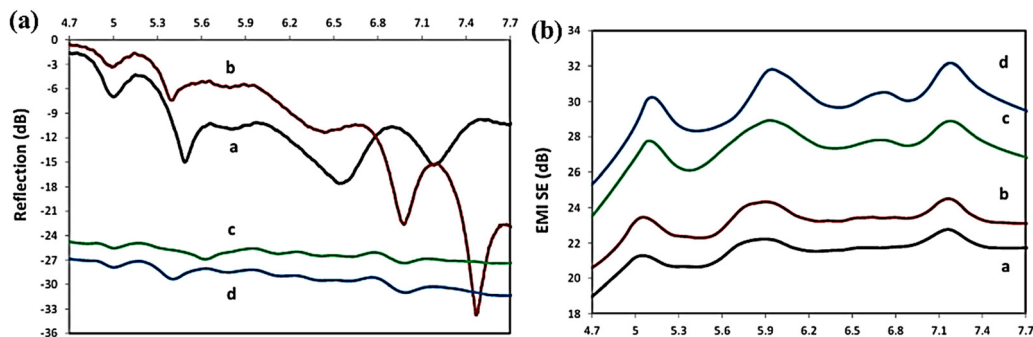
Fig. 3 (a) EM reflection and (b) EMI-SE of the samples: a. COOH-MWCNTs, b. PPy-MWCNT, c. PPy-MWCNT–Ag obtained by chemical reduction, and d. PPy-MWCNT–Ag prepared by UV reduction.[46]

of the sharp peak produced by the earlier sample, with interestingly minimum fluctuations in the PPy-MWCNT–Ag samples. PPy-MWCNT–Ag composites prepared by UV reduction showed the highest EM reflection among other samples at 27 dB to 30 dB with no fluctuations. The EMI-SE values of the COOH-MWCNT samples were in the range of 19–22 dB, while the PPy-MWCNT composite exhibited values in the range of 20–23 dB, the PPy-MWCNT–Ag samples showed values ranging from 23.5–28.5 dB, and PPy-MWCNT–Ag prepared by UV reduction (chemical reduction) had values of 25.5–31.5 dB (Fig. 3(b)). Among all the composites the PPy-MWCNT–Ag prepared by UV reduction showed the maximum shielding efficiency of ∼31.5 dB in the frequency range of 4–8 GHz. EMI-SE is dependent on various parameters, like the electrical conductivity, the thickness of the samples, the dimension, and the geometry in the frequency range of interest. The authors demonstrated that a higher concentration of silver in the UV-reduced PPy-MWCNT–Ag sample significantly enhanced the mobile charge transfer, leading to a notable increase in the EMI shielding effectiveness.[46]

Pasha *et al.* synthesized highly conductive nanocomposites consisting of PPy and manganese–iron oxide (MnFe$_2$O$_4$), treated with *para*-toluene sulfonic acid (PTSA) and introduced into a polydimethylsiloxane (PDMS) matrix to create a versatile hybrid structure.[47] The integration of the PTSA-treated PPy–MnFe$_2$O$_4$ nanoparticles formed an exceptional conductive network, elevating the electrical and magnetic properties of the composites. The PDMS-based nanocomposite displayed a remarkable electrical conductivity of 24.03 S cm^{-1}, complemented by robust mechanical properties, including a Young's modulus of 0.93 MPa and a tensile strength of 2.62 MPa. Due to the enhanced conductivity and magnetic characteristics, this PDMS-based nanocomposite, with a thickness of 0.5 mm, demonstrated superior electromagnetic shielding performance, particularly in X-band microwave frequencies, where it achieved an outstanding EMI shielding effectiveness (EMI-SE) of −21 dB, corresponding to 99.21% shielding efficiency. Furthermore, these nanocomposite shields exhibited excellent stability in terms of conductivity and EMI-SE values even when subjected to mechanical stretching and bending.

To enhance the magnetic losses in the composite material, Fe$_3$O$_4$ nanoparticles were incorporated in to composites as they possess a high magnetization, small size, corrosion resistance, environmental friendliness, and good economics,[48] due to which Sambyal *et al.* developed a composite material based on conducting polymers, which was enhanced with the inclusion of barium strontium titanate (BST), reduced graphene oxide (RGO), and Fe$_3$O$_4$ [BRF] nanoparticles at different weight ratios of monomers to BRF materials, and these samples were designated as PBRF1 (0.5∶1), PBRF2 (1∶1), and PBRF3 (1∶2). This enhancement was achieved through a chemical oxidative polymerization process of pyrrole. Then the resulting composite materials were characterized using various techniques, such as SEM, FT-IR, XRD, TGA, and VSM, as shown in Fig. 4. The addition of these filler materials into the conducting polymer matrix led to a significant improvement in its shielding effectiveness, particularly in the X-band frequency range of 8.2–12.4 GHz. All the data values related to the shielding are shown in Table 1.

This absorption-dominated shielding effectiveness value reached an impressive 48 dB, as shown in Fig. 5. Furthermore, the incorporation of dielectric and magnetic fillers notably enhanced the thermal and chemical stability of the composite material. Notably, the achieved shielding effectiveness value far surpassed the recommended limit of 30 to 40 dB for commercial applications, making these composite materials a highly effective solution for shielding against electromagnetic pollution.[49]

Utilizing an *in situ* polymerization technique, Kadar *et al.* synthesized composites of PPy/ZnWO$_4$.[50] The formation of these composites was validated through various characterization techniques, specifically XRD, FT-IR, and SEM. The composite network could be formed effectively due to the harmonious compatibility of the PPy matrix and the dispersant. This compatibility facilitated tunable charge transfer between PPy and ZnWO$_4$, resulting in synergistic effects. The inclusion of ZnWO$_4$ within the PPy matrix led to notable alterations in its electrical conductivity and dielectric behavior, promoting the absorption-dominant EMI shielding efficiency. The EMI shielding performance of PPy/ZnWO$_4$ achieved a maximum efficiency of −20 dB, effectively attenuating 99% of the electromagnetic
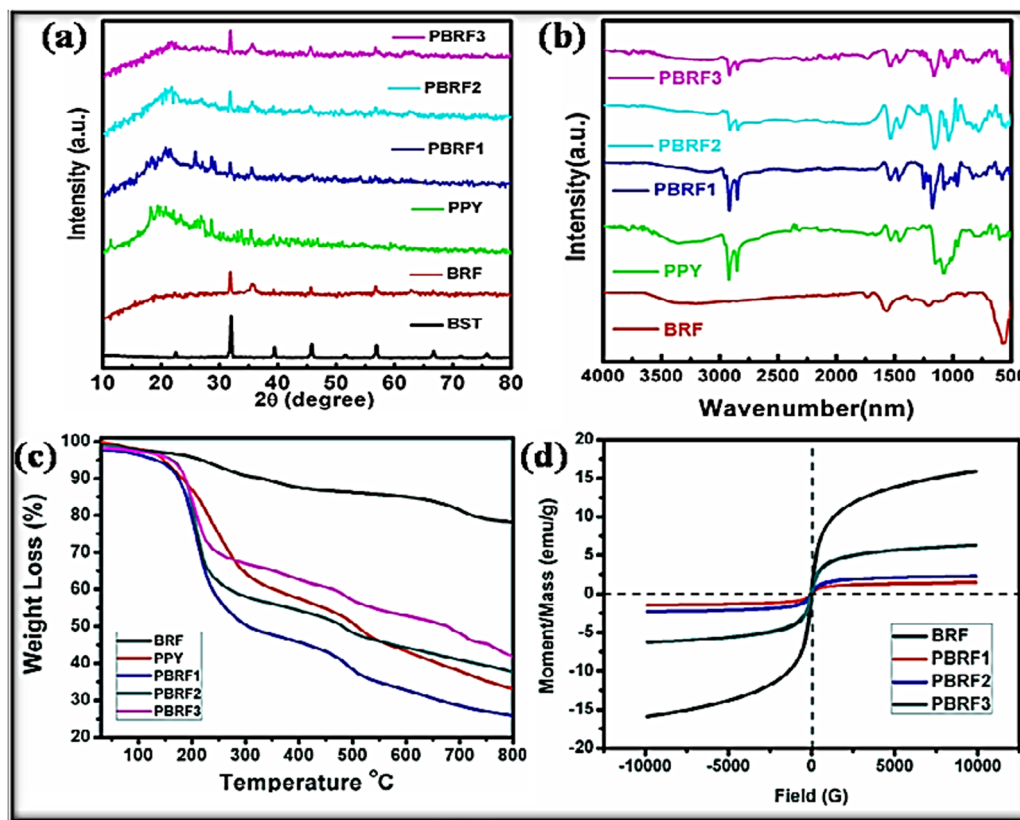
Fig. 4 (a) XRD patterns, (b) FT–IR spectra, and (c) thermogravimetric analysis (TGA) plots of BST, BRF, PPY, PBRF1, PBRF2, and PBRF3 composites in a N_2 atmosphere. (d) Vibrating sample magnetometer plots of the BRF and PBRF composites.[49]

Table 1 EMI shielding data of various combinations of BRF composites incorporated in a polypyrrole matrix

S. no.	Sample	Pyrrole (g)	BRF (g)	SE_T	SE_A	SE_R
1	BRF	—	—	14.06	12.22	1.84
2	PBRF1	6.79	3.35	44.44	38.47	5.97
3	PBRF2	6.79	6.79	44.56	41.36	3.20
4	PBRF3	6.79	13.58	48.58	42.75	5.83

noise. This level of shielding is particularly well-suited for practical applications within the X-band frequency range (8–12 GHz), which is of great relevance.

A multi-layered approach involving a hydrothermal technique and *in situ* chemical oxidative polymerization of the pyrrole monomer for the formation of a functionalized NiO/C/PPy nanomaterial, tailored for applications in electromagnetic shielding, was synthesized by Anwar *et al.* Impedance spectroscopy was employed to analyze the electrical behavior of a NiO/C/PPy pellet, with a specific focus on the variations in relaxation time with frequency under different temperatures. Notably, semiconductor-to-metal transition (SMT) was observed at 328 K within the NiO/C/PPy composite, elucidating the conduction mechanism through a carrier-hopping transport model involving Ni^{2+} and Ni^{3+} ions. The activation energy value ($E_a \approx$ 0.32 eV), as determined from impedance, conductivity, and dielectric measurements, highlighted the coherence between

the relaxation and conduction processes within the electro-active region. Furthermore, employing the variable range hopping (VRH) model, a localization length of carriers was calculated to be 1.56 Å. The NiO/C/PPy sample exhibited enhanced conductivity and low dielectric values, which are crucial for effective electromagnetic interference (EMI) shielding. Consequently, the composite material demonstrated a substantial electromagnetic interference shielding effectiveness of 21.9 dB in the X-band frequency range, establishing it as a promising candidate for high-frequency shielding applications.[51] Highly conductive nanocomposites consisting of PPy/manganese–iron oxide ($MnFe_2O_4$) treated with *para*-toluene sulfonic acid (PTSA) were incorporated into a polydimethylsiloxane (PDMS) matrix to create a versatile hybrid structure. The integration of the PTSA-treated PPy–$MnFe_2O_4$ nanoparticles formed a robust conductive network, enhancing both the electrical and magnetic properties of the composites. The PDMS-based nanocomposite demonstrated outstanding conductivity, reaching 24.03 S cm^{-1}, along with impressive mechanical characteristics, such as a Young's modulus of 0.93 MPa and tensile strength of 2.62 MPa. This nanocomposite, with a thickness of 0.5 mm, exhibited superior EMI performance dominated by absorption, achieving an EMI shielding effectiveness (EMI-SE) of −21 dB, corresponding to 99.21% shielding efficiency, particularly for X-band microwave frequencies. Furthermore, these nanocomposite shields displayed remarkable stability in conductivity
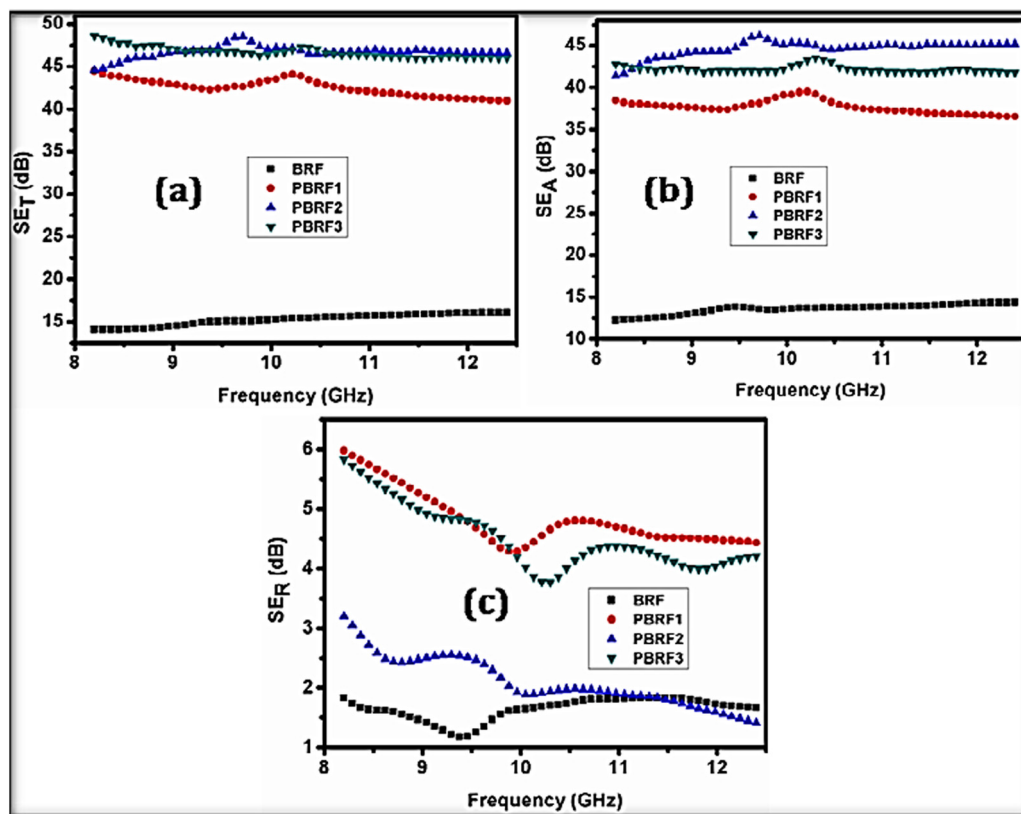
Fig. 5   (a) Variation of the total shielding effectiveness of the BRF and PBRF composites with the frequency, (b) shielding effectiveness due to absorption loss, and (c) shielding effectiveness due to reflection loss.[49]

and EMI-SE values even under mechanical stretching and bending, showcasing their durability. With their lightweight, flexible, and stretchable nature, coupled with high conductivity and superior EMI-SE, these composites hold significant potential for applications in flexible and foldable devices as intelligent wrap-on shields.[47]

PPy/Al$_2$O$_3$ nanocomposites were synthesized by Trung *et al.* through a chemical process, with their nanoscale morphology revealed by SEM and TEM analysis. These composites featured aluminum oxide cores enveloped by a thin PPy shell. The chemical structure of PPy within the nanocomposites was characterized by FT-IR and Raman spectroscopy. Notably, the PPy/Al$_2$O$_3$ nanocomposites exhibited properties akin to PPy films prepared through electro-polymerization on metal electrodes. Thermal analysis revealed that PPy within the nanocomposites remained stable even at temperatures as high as 521 °C. However, when assessing the shielding effectiveness of the PPy nanocomposite-coated fabric within the 8–12 GHz range, it only showed a modest attenuation value of approximately −3.3 dB (53%), which may not be sufficient for industrial applications. To make these nanocomposites suitable for practical use, improvements in their shielding effectiveness are imperative.[52] To increase their shielding effectiveness, Yang *et al.* synthesized graphene (GN)/PPy/Al$_2$O$_3$ ternary aerogels as an advanced membrane filler for a synergistic enhancement of the thermal conductivity, EM wave absorption, and electrical

insulation. A few graphene and PPy (3–5 wt%) particles with thermal conduction and electric conductivity properties were uniformly dispersed in Al$_2$O$_3$ nanoparticles, which were characterized by their thermal conduction and electrical insulation capabilities. This dispersion created multiple polarizations and established an effective heat conducting but electrically insulating pathway for phonon transmission. Consequently, the GN/PPy/Al$_2$O$_3$ ternary aerogels (1 : 1 : 15, 50% loading) exhibited a wide absorption frequency band (6.48 GHz, 2.0 mm thickness), high thermal conductivity (4.649 W mK^{-1}), and excellent electrical insulation (σ = 0.0282 S m^{-1}). Remarkably, their thermal conduction and microwave absorption capabilities significantly surpassed those of most reported fillers.[53]

Environmentally friendly carbon aerogels derived from cellulose (CDCA) utilized as a porous substrate for the integration of α-Fe$_2$O$_3$ and PPy through a process involving pyrolysis and vapor-phase polymerization were synthesized by Wan *et al.* SEM and TEM were applied and revealed well-dispersed wrinkled PPy sheets and α-Fe$_2$O$_3$ nanoparticles within the CDCA matrix. The strong interactions between the oxygen-containing groups of CDCA and the nitrogen lone pairs of PPy (or the oxygen components of α-Fe$_2$O$_3$) were confirmed by FT-IR and XPS analysis. When employed as materials for shielding against electromagnetic interference (EMI), the composite comprising α-Fe$_2$O$_3$/PPy/CDCA (referred to as FPCA) exhibited the highest overall shielding effectiveness (SE$_{total}$) at 39.4 dB. This SE$_{total}$

value was approximately 2.0 times greater than that of acid-treated CDCA (19.3 dB), 2.9 times greater than that of PPy (13.6 dB), and 1.3 times greater than that of α-Fe$_2$O$_3$/CDCA (29.3 dB). These remarkably increasing trends reflected that the existence of α-Fe$_2$O$_3$ and PPy effectively facilitated the improvement of the EMI shielding property of the composites. Notably, the shielding effectiveness attributed to absorption accounted for a significant portion (ranging from 78.2% to 84.2%) of the SE$_{total}$ for FPCA, indicating that the absorption-dominant shielding mechanism played a crucial role in mitigating secondary radiation.[54] From the above results, it can be seen that the SE$_{total}$ value of FCPA was comparable to or even slightly higher than that of previously reported carbon-based EMI shielding materials, such as exfoliated few layer graphene[55] (12 dB), carbon fiber/silica[56] (12.4 dB), and biomorphic porous carbon[57] (37 dB). Using green tea extract as a reducing and stabilizing agent, Patel and co-workers used *in situ* polymerization to create iron nanoparticles (FeNPs) embedded in polypyrrole (PPy/Fe) with tellurium oxide (PPy/Fe@TeO$_2$) nanocomposites.[58] Utilizing a redox reaction between PPy/Fe, TeO$_2$, and green tea extract, the iron nanoparticles were uniformly implanted with varying concentrations (5–25 wt%) of TeO$_2$ (PPy/Fe@TeO$_2$) as ternary nanocomposites on the surface of PPy. This process is known as *in situ* functionalization. Electromagnetic shielding interference (EMI) and electrical conductivity (both DC and AC) were noted. The outcomes demonstrated that when the weight percentage of TeO$_2$ in the composite was reduced, the DC conductivity increased. From 303 to 378 K, there was a minor increase in DC conductivity as well. The conductivity is determined by the number of available charge carriers and their mobility. It was found that the mobility of charge carriers increased with increasing temperature, which led to an increase in sample conductivity. Furthermore, it was shown that the alternating current (AC) conductivity of PPy/Fe@TeO$_2$ increased with frequency; however, this phenomenon was more pronounced in the composite with 15 wt% TeO$_2$. The higher dielectric values for the 15 wt% TeO$_2$ ternary nanocomposites could be attributed to the efficient charge-transfer process within the polymer matrix, leading to the accumulation of charge carriers. Due to the polymerization, the charge transfer of TeO$_2$ NPs decreased with increasing the TeO$_2$-doping concentration. The dissipation of charge from the polymer complex resulted in the dielectric loss factor (imaginary part of the dielectric). Hence, the composite with the 15 wt% TeO$_2$ sample exhibited the greatest performance loss between the 2.0 and 3.0 GHz frequencies when it comes to the EMI shielding performance compared to other materials.

Patel *et al.* decorated iron using an *in situ* polymerization to obtain PPy-fly ash nanocomposites with different fly ash compositions (5, 10, 15, 20, and 25 wt%).[59] Various spectroscopic techniques, including X-ray diffraction, scanning electron microscopy, FT-IR, and transmission electron microscopy, were used to confirm the morphological and structural features. As the concentration of fly ash grew, the samples' crystallinity increased as well, according to the X-ray diffraction analysis.

The homogeneous distribution and ornamentation of iron particles in the PPy-fly ash nanocomposites were verified using electron microscopy techniques. Measurements of the DC conductivity showed that the materials behaved as semiconductors. The efficiency of the as-prepared composites EMI shielding was studied in the microwave region's S-band, or frequency range of 2 to 3 GHz. The findings of the EMI shielding effectiveness tests showed that, compared to the other composites, the 25 wt% Fe-PPy–FA composite absorbed higher power. Ganguly *et al.* synthesized PPy/GNFs/IONPs on non-polar plastic *via* surface chemistry. The fabrication process entailed three sequential steps: first, corona-treated PP films underwent silane treatment to coat them with a thin layer of silica. Subsequently, the silicate PP films were coated with a mixture of pyrrole, GNFs, and IONPs, followed by exposure to UV light. The resulting films exhibited a surface conductivity around ≈20 S cm^{-1} at room temperature. Additionally, a ≈15-micron thickness of the coated film demonstrated effective shielding against electromagnetic waves in the X-band region (8.2–12.4 GHz), with a confirmed shielding effectiveness of approximately 24 dB.[60]

Varshney *et al.* synthesized a stick-shaped polypyrrole nanocomposite, adorned with γ-Fe$_2$O$_3$ using the microemulsion method. The morphology was controlled by lauryl sulfate, which facilitated the formation of self-assembled micelles, ultimately resulting in the formation of nano-sticks. The incorporation of γ-Fe$_2$O$_3$ into the conducting matrix introduced a new class of composite materials with enhanced microwave-absorption properties, achieving a total shielding effectiveness of 28.4 dB (with an SE$_A$ at 22.6 dB and SER at 5.8 dB). Magnetic studies revealed that these conducting ferromagnetic nanocomposites exhibited a high saturation magnetization (M_s) value of 35 emu g^{-1} and conductivity in the order of 10^{-2} S cm^{-1}. The addition of γ-Fe$_2$O$_3$ nanoparticles resulted in increased interfacial dipolar polarization and higher anisotropic energy, owing to their nano-size, which consequently contributed to the elevated levels of shielding effectiveness. Fig. 6(a) and (b) show the behaviors of the real and imaginary parts of the permittivity of the PPy–Fe$_2$O$_3$ composites across varying frequencies, while Fig. 6(c) and (d) illustrate the variation of the real and imaginary parts of the magnetic permeability of the same composites as a function of the frequency. The dependence of the shielding effectiveness on the magnetic permeability suggests that optimal absorption values can be achieved for materials exhibiting moderate conductivity and magnetization. Notably, the high electromagnetic interference shielding effectiveness could be predominantly attributed to an absorption mechanism rather than reflection.[61]

A quaternary nanocomposite of Epoxy–PPy/Fe$_3$O$_4$–ZnO (1:2, 1:1, 2:1) was created and its ability to absorb X-band microwaves was examined by Olad *et al.* The application of conducting PPy and metal oxides simultaneously in the epoxy matrix was tested in an effort to boost the X-band region's microwave absorption intensity and broadness. An assessment was conducted on the combined impact of iron oxide and zinc oxide nanoparticles with varying the weight ratios (Fe$_3$O$_4$/ZnO) on
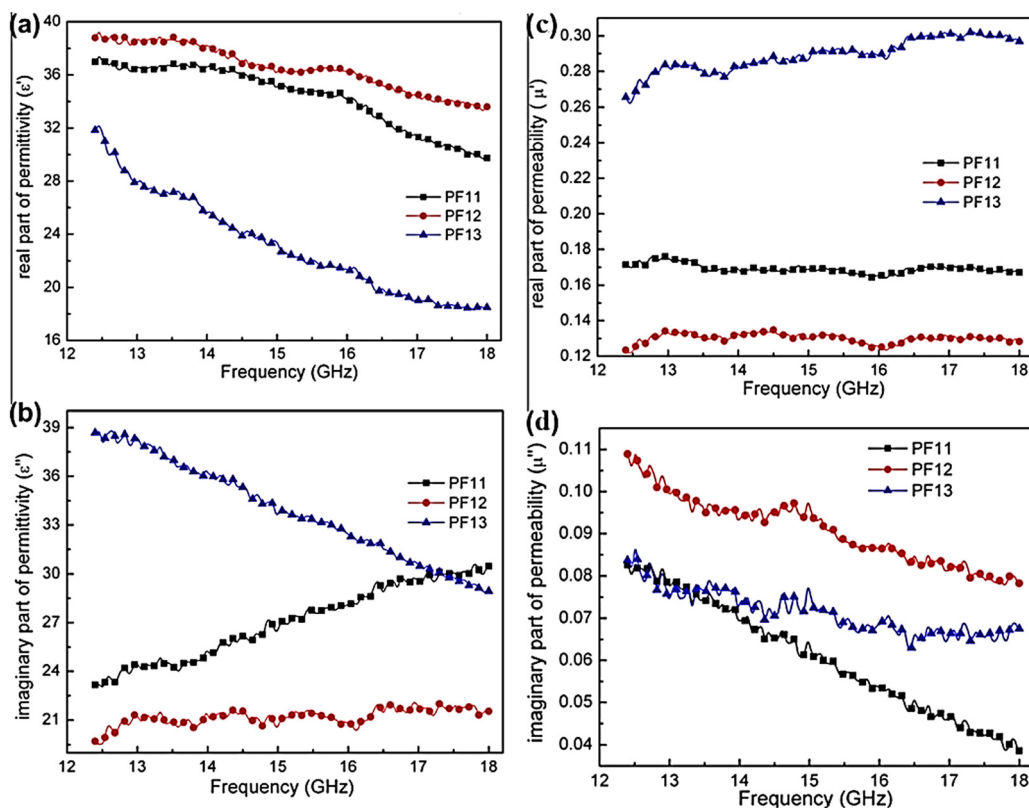
Fig. 6 Behavior of the (a) real and (b) imaginary parts of the permittivity of the PPy–Fe$_2$O$_3$ composites as a function of the frequency. Variation of the real (c) and (d) imaginary parts of the magnetic permeability of the PPy–Fe$_2$O$_3$ composites as a function of the frequency.[61]

electromagnetic wave absorption. A vector network analyzer was used to assess the electromagnetic properties inside the X-band region, or 8.2–12.4 GHz, which would be suitable for radar applications. The results of the electromagnetic wave absorption showed that the Epoxy–PPy/Fe$_3$O$_4$–ZnO quaternary nanocomposite had a large absorption area and high attenuation. This is thought to be because of the components' synergistic effects, the magnetic loss factor of Fe$_3$O$_4$, and the dielectric loss characteristics of PPy. The greatest reflection loss was around 32.53 dB at 9.96 GHz for Epoxy–PPy/Fe$_3$O$_4$–ZnO when the nanocomposite had a thickness of 2 mm and an iron oxide to zinc oxide ratio of 2 : 1. The absorption bandwidth, which covered the frequency range of 8.2–12.4 GHz, was up to 4.2 GHz with a reflection loss of less than ∼10 dB (90% attenuation). The absorber with the best reflection loss qualities with the Epoxy–PPy/Fe$_3$O$_4$–ZnO nanocomposite with a 2 : 1 iron oxide to zinc oxide ratio was found to have 15% (w/w) PPy/ epoxy resin. The produced nanocomposites' dielectric loss tangent and magnetic loss tangent values ranged from 0.25 to 0.7 and 0.08 to 0.09, respectively, and are depicted in the loss curves in Fig. 7. Dielectric loss was thus most likely the mechanism responsible for the absorption of microwaves.[40]

By combining the sol–gel procedure with the self-combustion technology, nanocomposites of CoCe$_{0.05}$Fe$_{1.95}$O$_4$–PPy with magnetic and microwave-absorbing capabilities were synthesized by Ahmad et al., as shown in Fig. 8.[62] The nanocomposites were found to consist of a single spinel phase, with

no contaminants discovered, as indicated by the X-ray diffraction measurements. The ferromagnetic nature of the nanocomposites was demonstrated via the hysteresis loop. To assess the magnetic properties, measurements were made of the saturation magnetization, cation distribution, alternating current susceptibility, and Curie temperature. The permittivity (ε', ε'') changed with the frequency in accordance with interfacial polarization of the Maxwell–Wagner type. The microwave permeability's real and imaginary components peaked at lower frequencies and then diminished as the frequency rose. Due to its superparamagnetic behavior, the composite showed potential for application in shielding techniques.

PPy–CaCu$_3$Ti$_4$O$_{12}$–CoFe$_2$O$_4$ (PPy–CCTO–CFO) nanocomposites were successfully synthesized through an in situ chemical oxidative polymerization process by Dhugga et al. These nanocomposites were formulated with varying ratios of pyrrole monomer to CCTO and CFO; specifically, with the weight ratios of 1 : 0.5 : 0 (referred to as PC5F0), 1 : 0.5 : 0.1 (referred to as PC5F1), and 1 : 0.5 : 0.3 (referred to as PC5F3). Detailed investigations using IR and XRD techniques confirmed the effective integration of CCTO and CFO into the PPy matrix. Analysis of the surface morphology revealed a distinctive cup-like structure, which was a result of interfacial interactions within the nanocomposites. Notably, the PC5F3 nanocomposite exhibited an outstanding total shielding effectiveness of approximately 30 dB, corresponding to a remarkable 99% attenuation of microwaves. This exceptional shielding performance was
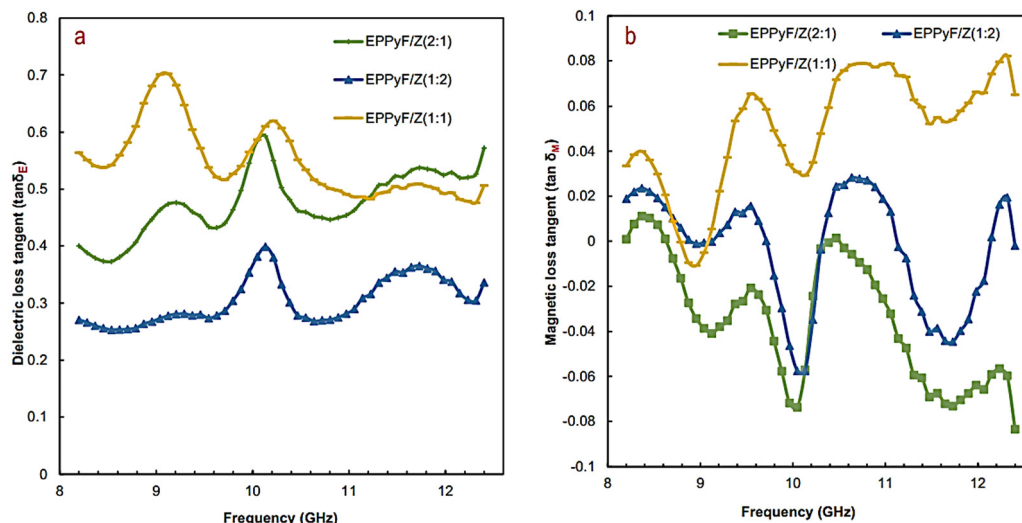
Fig. 7 Frequency dependence of the dielectric loss tangent of the EPPyF/Z nanocomposite sample with Fe_3O_4 to ZnO ratios of 1:2, 1:1, and 2:1. (a) Magnetic loss tangent of EPPyF/Z nanocomposite samples with Fe_3O_4 to ZnO ratios of 1:2, 1:1, and 2:1 (b).[40]
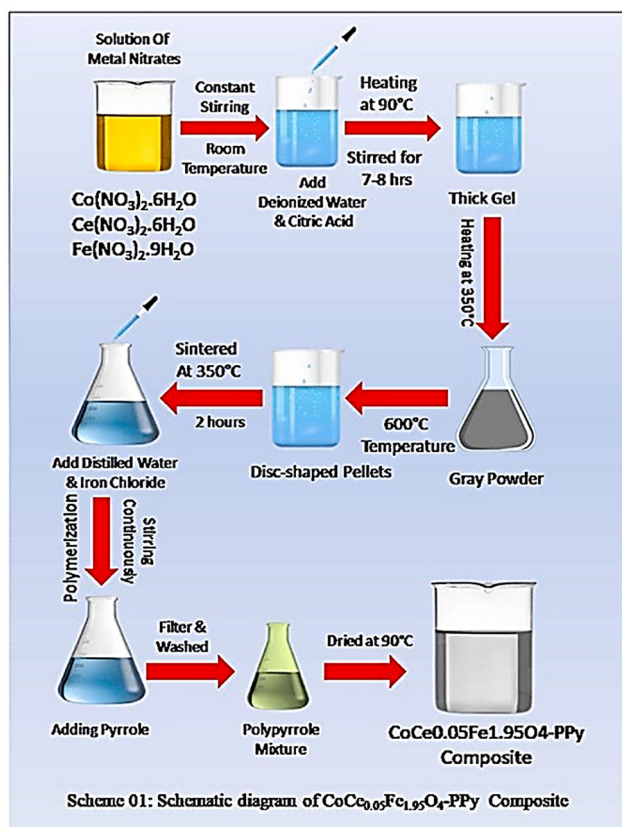

Fig. 8 Schematic diagram of the $CoCe_{0.05}Fe_{1.95}O_4$–PPy composite preparation process.[62]

achieved through a combination of absorption effectiveness (SE ∼ 22 dB) and minimal reflection (∼8 dB). The absorption efficiency of the PC5F3 nanocomposite was found to be approximately 99%, as shown in Fig. 9. The increase in absorption efficiency and shielding effectiveness observed in the

PC5F3 nanocomposite could be attributed to the synergistic effects of the dielectric and magnetic losses, as well as contributions from free charges in the interfacial layer, interfacial polarization, and the wedge effect.[63]

Novel hierarchical core–shell structures prepared by combining Fe_3O_4 nanoparticles (NPs) and conductive PPy coating on collagen fibers (CFs) were synthesized by Liu et al., as shown in Fig. 10,[64] with the formation of a composite material with exceptional electromagnetic wave (EMW)-absorption properties. The $CF/Fe_3O_4/PPy$ nanocomposite, as developed, could effectively dissipate incident EMW energy through multiple mechanisms, including dielectric loss, magnetic loss, and interfacial polarization loss. Additionally, the unique hierarchically supra-fibrillar structure of the CFs, which incorporated nano- to microscale pores, induced the multiple reflection and scattering of EMWs. This feature significantly enhanced the EMW attenuation capacity of the Fe_3O_4 NPs and PPy coated onto the CFs by providing multiple transmission routes for the EMWs. As a result of these design innovations, the $CF/Fe_3O_4/PPy$ nanocomposite exhibited an outstanding shielding effectiveness value (SE) of approximately 72.0 dB, with a substantial absorption contribution of 85.8%. The specific SE reached 360 dB cm^2 g^{-1}. Notably, the $CF/Fe_3O_4/PPy$ nanocomposite demonstrated impressive radar-stealth performance within the frequency range of 8.2–11.5 GHz, with a reflection loss exceeding −10.0 dB and reaching up to a −23.7 dB reflection loss. This performance could be adjusted by varying the proportion of Fe_3O_4 NPs and PPy coated onto the CFs.

Varshney et al. explored the potential use of industrial byproduct fly ash in the development of nanostick-shaped polypyrrole composites, decorated with γ-Fe_2O_3 and fly ash particles, using an in situ emulsion polymerization.[65] The investigation focused on evaluating the structural, magnetic, and electromagnetic shielding properties of these composites with varying the concentrations of γ-Fe_2O_3 and fly ash particles.
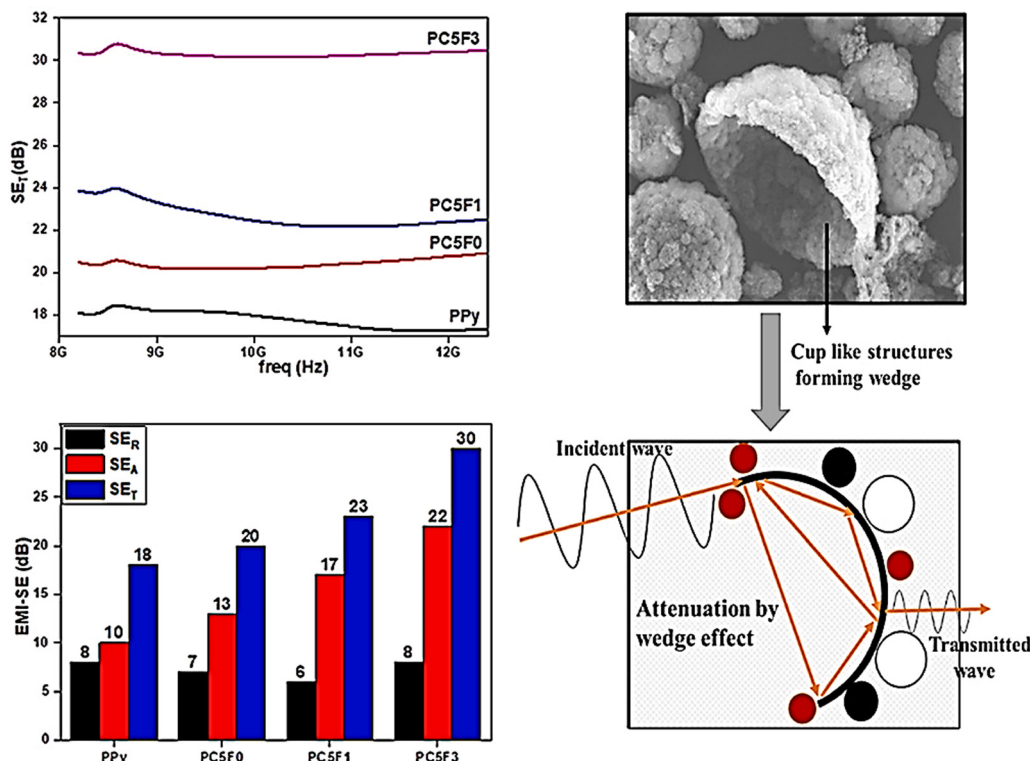
Fig. 9 Graphical abstract showing results for the analysis and tests of PPy–CaCu$_3$Ti$_4$O$_{12}$–CoFe$_2$O$_4$.[63]

The results suggested that by adjusting the concentration of the constituents within the polymer matrix, the properties of the composites could be optimized. The PPy–γ-Fe$_2$O$_3$-fly ash nanocomposites exhibited a superparamagnetic behavior with an M_s value of 13.55 emu g^{-1}, and electrical conductivity around 10^{-2} S cm^{-1}, and achieved a maximum shielding effectiveness (SE$_A$(max)) of approximately 17.4 dB due to

absorption. Moreover, an overall shielding effectiveness (SE = SE$_A$ + SE$_R$) of up to 25.5 dB ($\sim$99.7% attenuation) was observed for the polypyrrole nanocomposites containing pyrrole, γ-Fe$_2$O$_3$, and fly ash in a 1 : 1 : 0.5 wt. ratio, within the frequency range of 12.4–18 GHz (Ku-band). Benzoui et al.'s work contributes to the understanding of how flexible polypyrrole–silver nanocomposite films with a changed silane surface affect the
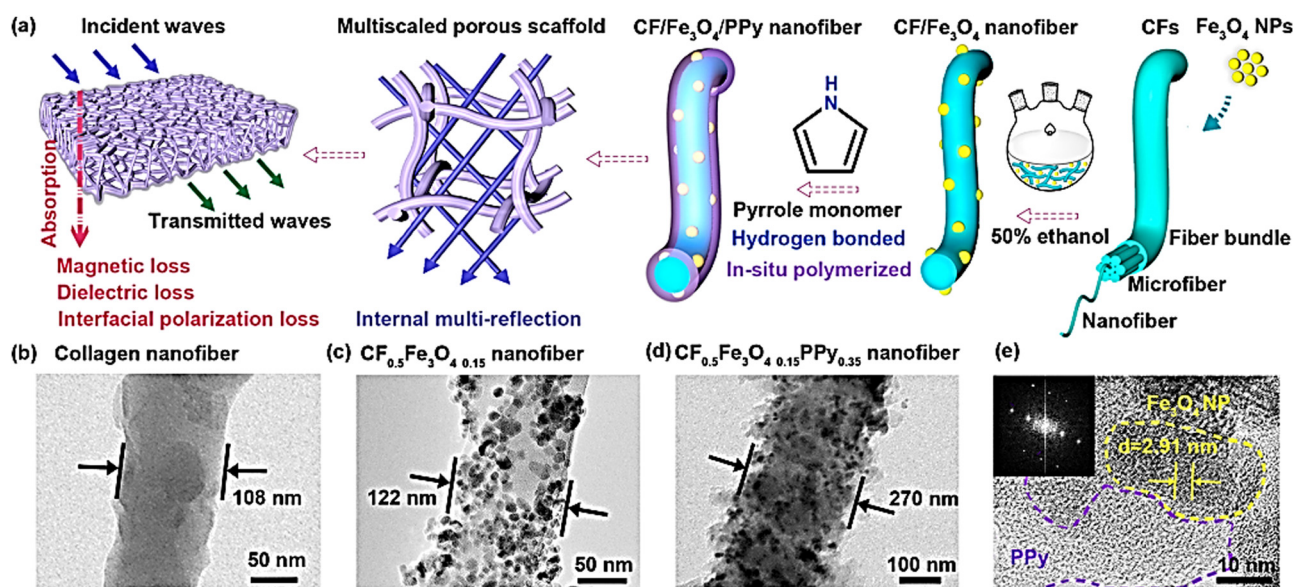

Fig. 10 Schematic illustration of the novel hierarchical core−shell structure prepared by combining Fe$_3$O$_4$ nanoparticles (NPs) and a conductive PPy coating on collagen fibers (CFs).[64]

effectiveness of electromagnetic interference shielding (EMI-SE). Thus, UV polymerization was used to *in situ* deposit PPy–Ag on biaxial oriented polyethylene terephthalate (BOPET) flexible substrates whose surfaces were treated by 3-amino-propyltrimethoxysilane (APTMS). The structural, morphological, thermal, and electrical characteristics of the prepared films were correlated with the effects of the substrate surface treatment. Thereafter, EMI-SE measurements of the elaborated films were carried out as per ASTM D4935 standard for a wide frequency band extending from 50 MHz to 18 GHz. The obtained results confirmed that the APTMS-treated BOPET film exhibited a higher EMI shielding performance and better electrical characteristics compared to the untreated film. In fact, a 32% enhancement of the EMI-SE was noted for the treated films compared to the untreated ones.[66]

Zhao and co-workers established a straightforward and durable synthesis pathway for creating a multilayer structured composite of cuprammonium fabric/polypyrrole/copper (CF/PPy/Cu).[67] This composite showed promising potential as an electromagnetic interference (EMI) shield, combining attributes of both electromagnetic wave absorption and reflection. The preparation process involved a direct deposition of the PPy layer onto the bare CF substrate through an *in situ* polymerization approach. The interaction between PPy and the CF substrate was examined using FT-IR and FT-Raman measurements, which revealed a hydrogen bonding interaction between PPy (–N–H) and the CF ($>$C–OH) substrate. Subsequently, a Cu film was formed on the PPy-coated CF (CF/PPy) using an electroless copper plating method. Elemental analysis at each step was conducted through XPS measurements, while XRD analysis confirmed the FCC crystalline structure of the top Cu film. The obtained SEM images demonstrated that the PPy film had an average thickness of approximately 1.52 μm with a deviation of 11.4%, facilitating interfiber connection. The growth mechanism of the top Cu films was proposed based on their surface morphologies, as shown in Fig. 11. The shielding effectiveness (SE) values were compared for the copper-plated CF (CF/Cu) and CF/PPy/Cu using a spectrum analyzer (30–1000 MHz). The resulting CF/PPy/Cu composite exhibited superior EMI-SE (30.3–50.4 dB) with a sheet resistance of 85.8 mΩ sq^{-1}. Further analyses, including ultrasonic washing, TGA, and tensile measurements, confirmed the excellent serviceability of the proposed conductive fabric, making it reliably suitable for practical applications.

In situ polymerization was employed to create nanocomposites of iron-decorated PPy-stannic oxide (5, 10, 15, 20, and 25 wt%) by Patel *et al.* AC and DC electrical conductivity as well as the electromagnetic shielding interference (EMI) properties were assessed. The findings indicated that the conductivity exhibited an upward trend with a reduction in the weight percentage of SnO$_2$ nanoparticles. Furthermore, a marginal increase in DC conductivity was observed within the temperature range of 303 K to 378 K. Among the composites, the Fe-PPy-5% SnO$_2$ sample displayed a slightly lower resistance as it had more mobile charge carriers which interact with EM radiation, hence the shielding by reflection increased. The dielectric
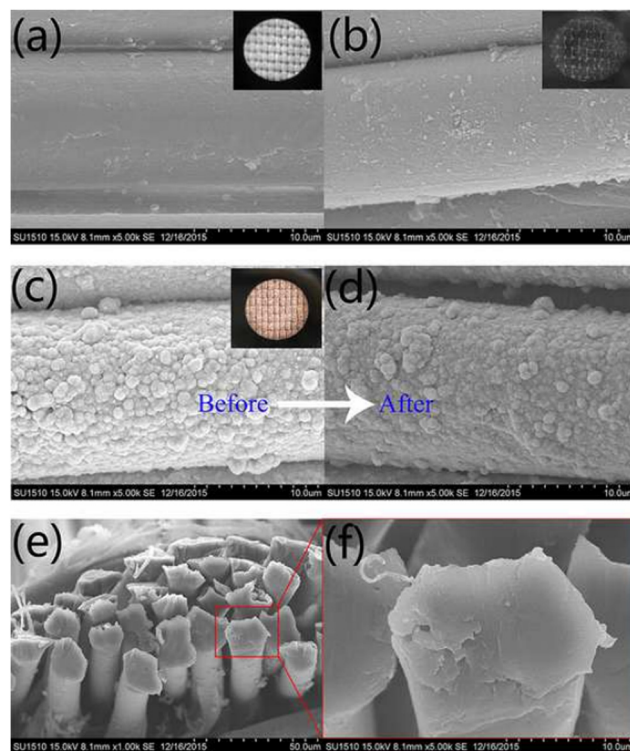

Fig. 11 SEM images of (a) bare CF and (b) after PPy deposition. (c) and (d) SEM images of CF before and after PPy deposition. (e) and (f) PPy coating and zoomed in image of a filament.[67]

constant demonstrated a decrease with increasing frequency, with Fe-PPy-5% SnO$_2$ exhibiting the maximum value and Fe-PPy-25% SnO$_2$ the minimum. Remarkably, the Fe-PPy-5% SnO$_2$ sample demonstrated the highest shielding effectiveness in the 2–3 GHz frequency range compared to the other composites. These experimental outcomes underscore the promising properties of the materials, particularly in terms of EMI shielding, suggesting potential applications in electronic, electrical, and EMI shielding scenarios.[68]

A series of composites, including PNT/GO, PNT/GO-Fc, PNT/GO-Fc-GO, PNT/GO-EDA-Fc, and PNT/GO-EDA-Fc-EDA-GO, were synthesized through *in situ* chemical oxidative polymerization by Lin *et al.* The EMI shielding performance of these polypyrrole nanotube/ferrocene-modified graphene oxide composites was evaluated across the frequency range of 1.0–4.5 GHz. The findings revealed that the incorporation of 50 wt% of the PNT/GO-EDA-Fc-EDA-GO-7 : 1 composite into the paraffin matrix resulted in a shielding effectiveness of 28.73 dB, with a conductivity of 1.320 S cm^{-1}, compared to the lower values for PNT/GO-EDA-Fc-EDA-GO-3 : 1 (0.77 S cm^{-1}), PNT/GO-EDA-Fc-EDA-GO-5 : 1 (0.56 S cm^{-1}), and PNT/GO-EDA-Fc-EDA-GO-9 : 1 (0.48 S cm^{-1}). This enhancement could be attributed to the formation of a robust π–π stacking system by GO-EDA-Fc-EDA-GO, along with interactions between PNT and GO-EDA-Fc-EDA-GO, such as π–π stacking, hydrogen bonding, and electrostatic forces, which facilitated electronic transition and accelerated electron transmission within the

composite material. Additionally, the interface polarization between the dipole polarization and heterogeneous interfaces further increased the EMI shielding performance of the composite. In conclusion, the synthesized PNT/GO-EDA-Fc-EDA-GO-7 : 1 composite exhibited significant promise for applications in EMI shielding.[69] Rashmi *et al.* synthesized freestanding PPy–PVA/Ni (1, 2, 3, 4, and 5) ternary composites by an *in situ* chemical oxidative polymerization of pyrrole and PVA as a binder using APS as an oxidizing agent and coated with different concentrations (0.01, 0.02, 0.03, 0.04, and 0.05 M) of Ni^+ ions using *Adathoda vasica* leaf extract as a reducing agent. The effect of the PPY-PVA/Ni nanocomposites on the electrical and EMI shielding properties of the nanocomposites was studied. The crystal structure of the dopant (Ni nanoparticles), thermal degradation, and morphology of these composites were characterized by XRD, FESEM, and TG analysis. The maximum electrical conductivity (4.2×10^{-4} S cm^{-1}) was also achieved by doping the PPY-PVA binary composites with 0.01 M Ni^+ ions to form PPY-PVA/Ni-1 ternary nanocomposites. This significant increase in electrical conductivity achieved an EMI shielding effect of up to $\sim$16.5 dB in the frequency range from 2.1–3 GHz (S-band). The increases in electrical conductivity and EMI shielding for the composites with the hybrid fillers (PPY-PVA/Ni) demonstrated the synergistic benefits of such fillers when used together.[70]

Silver/polypyrrole/polyvinylalcohol (Ag/PPy/PVA) polymer nanocomposite films were synthesized by Srivastava *et al.* through an *in situ* polymerization of pyrrole, incorporating varying concentrations of silver nanoparticles ranging from 0.5% to 10%. The resulting conductive films exhibited flexibility, lightweight properties, thermal stability, and a notable hydrophobicity/hydrophilicity ratio. X-Ray diffraction analysis indicated the formation of face-centered cubic (fcc) silver nanoparticles with sizes in the range of approximately 20–40 nm. UV-visible spectroscopy revealed distinctive bands corresponding to Ag nanoparticles and PPy within the copolymer nanocomposites. SEM studies of the nanocomposite films demonstrated a well-conjugated integration of the filler material into the polymer matrix. The electromagnetic shielding efficiency (EMI) of the films was assessed using a vector network analyzer. The Ag concentrations in the films varied between 0.5% to 10%. It was observed that when increasing the silver concentration and the thickness from 1 mm to 3 mm, the shielding efficiency increased in all the samples. The values of EMI shielding effectiveness for the various films are presented in Table 2.

From the table, it could be observed that the trend remained the same for the solution cast films but the values were 10% higher than for the 1 mm thick films. The higher values for the 3 mm thick films are considered to be due to two possible reasons: (i) the homogeneous thickness as well as particle distribution within the films and (ii) the thick non-porous surface of the film. Overall, it was observed that the 2% Ag-containing samples of 1 mm or 3 mm thickness showed the most consistent performance in terms of the interaction with electromagnetic waves and their retaining excellent EMI-SE. The maximum shielding effectiveness observed was in the range of -30 dB to -35 dB for the 5% and 10% Ag-loaded films while the average range for all the samples was 20–33 dB. The results obtained showed that the material thus formulated is a potential EMI shielding material and can also be used for commercial applications due to its ease of formation and simple processing.[71] Sun *et al.* synthesized two-dimensional graphene oxide@zero-dimensional polypyrrole/one-dimensional carbonyl iron fiber (GO@PPy/CIF) composites with a core–shell structure by a facile *in situ* chemical oxidative polymerization method, and then systematically studied their electromagnetic properties. It was indicated that when the mass ratio of GO@PPy to GO@PPy/CIF was 15 wt%, the optimal reflection loss reached -53.67 dB at 12.24 GHz with a 2.56 GHz effective absorption bandwidth ($R_L \leq -10$ dB), and the corresponding thickness was 2.13 mm. Additionally, the better impedance matching, large attenuation constant, and coupling effect of the dielectric-magnetic loss played a combined role in the optimized absorption.[72]

Ternary nanocomposites of polypyrrole/Fe_3O_4/graphene (PPy/Fe_3O_4/RGO) were synthesized using a two-step method by Xing and co-workers. Initially, PPy/Fe_3O_4 composites were anchored onto the GO surface *via* a chemical one-step process, followed by reducing GO. The electromagnetic wave absorption (EMWA) performance of these composites could be adjusted by varying the amount of pyrrole monomers. The PPy/Fe_3O_4/RGO-0.5 composite (with 0.5 mL pyrrole) achieved a maximum reflection loss of -66.0 dB at 14.88 GHz and an absorption bandwidth exceeding -10 dB over 5.76 GHz with a 2.5 mm absorber thickness. Studies on the electromagnetic absorbability indicated that the PPy/Fe_3O_4/RGO composites exhibit superior electromagnetic absorption properties compared to Fe_3O_4/RGO, primarily due to the improved impedance matching, enhanced interfacial effects, and geometric effects. This approach broadens the range of electromagnetic-wave-absorption materials, demonstrating that modifying graphene

Table 2 Shielding effectiveness of the films

% Ag	SE dB (maximum) 1 mm thick film	SE dB (average) 1 mm thick film	SE dB (maximum) 3 mm thick film	SE dB (average) 3 mm thick film
0.5	-19.04	-17.48	-19.94	-19.55
1.0	-21.68	-17.34	-26.56	-24.47
2.0	-22.83	-21.49	-28.86	-27.4
5.0	-32.49	-29.56	$\mathbf{-33.02}$	-30.52
10.0	-30	-29.73	$\mathbf{-35}$	-31.88

with PPy and Fe_3O_4 can endow the ternary nanocomposites with significant potential for future applications as electromagnetic-wave-absorption materials.[73]

Novel core–shell Fe_3O_4/C/PPy composites were synthesized by Shukla *et al.* using a hydrothermal and chemical oxidative polymerization method. The resulting Fe_3O_4/C/PPy composite displayed a dual core–shell structure, with an intermediate carbon layer facilitating the excellent electrical connectivity between Fe_3O_4 nanoparticles and PPy polymer. These trilaminar core/shell composites were then evaluated as electromagnetic interference (EMI) shielding materials to mitigate EMI pollution. Remarkably, Fe_3O_4/C/PPy (2:8 wt/wt) achieved an outstanding EMI shielding efficiency (> 28 dB) at a thickness of 0.8 mm, primarily driven by absorption mechanisms. Additionally, the magnetic properties of the Fe_3O_4/C/PPy composites were found to be crucial for their EMI absorption performance, with the content and thickness of the shell influencing the spin motion of the Fe_3O_4 nanoparticles. Consequently, it was anticipated that spin motion plays a pivotal role in the EMI shielding performance of Fe_3O_4/C/PPy composites.[74] Kanwal and co-workers synthesized PPy-coated carbon fibers (CFs), GO, and magnetite nanoparticles (MPs) embedded in epoxy to enhance both the mechanical properties and electromagnetic interference (EMI) shielding effectiveness (SE) of hybrid composites. To achieve this, PPy was applied onto desized woven carbon fiber mats *via* electrophoretic deposition. The graphene oxide and magnetite nanoparticles were synthesized using improved Hummers' and modified Massart's methods, respectively. Graphite oxide was transformed into GO through ultrasonication, revealing an average thickness of approximately 1.4 nm, as confirmed by atomic force microscopy (AFM). The hybrid composites containing CFPPy-0.2 wt% GO-0.2 wt% MPs demonstrated significant enhancements, with approximately 52%, 24%, 60%, and 25% increases in tensile strength, Young's modulus, toughness, and elongation, respectively, compared to the neat CF-epoxy composites. Moreover, all the hybrid composites in this study exhibited an SE exceeding 30 dB, positioning them as promising lightweight and high-strength materials for EMI shielding applications within the X-band frequency range.[10] Table 3 summarizes the microwave-absorption properties of some other current reported PPy-based absorbers.

4. Properties of polypyrrole nanocomposites for EMI shielding

Polymer-based nanocomposite materials exhibit various properties, such as magnetic and dielectric properties, that are useful for EMI shielding as described below.

4.1 Magnetic properties

Polymers do not have inherent active magnetic properties, but such properties are conceivable in the presence of a combination of conductive polymers and magnetic particles. The radiation in the microwave region includes both magnetic and electric fields, in which magnetic and electrical dipoles in the shield govern the wave absorption. The interaction between magnetic dipoles can result in the absorption of electromagnetic waves in the magnetic field. This is mostly dependent on the permeability ($\mu_r = \mu' - j\mu''$) within the shield. Real and imaginary permeabilities are related to the acquisition and loss of electrical energy, respectively. The use of magnetic nanoparticles can improve the permeability of a complex, thereby enhancing the absorption of electromagnetic waves connected to the magnetic field.[94–96]

4.2 Dielectric properties

Certain parameters, such as nanoparticle dispersion, matrix properties, intrinsic properties conductivity, matrix affinity in nanoparticles, and characteristic ratio of nanoparticles, govern

Table 3 Microwave absorption values of other reported PPy-based composites

Materials		Minimum R_L value		Filler content (wt%)			
		dm	$R_{L_{min}}$	dm		$R_L < 10$ dB	Ref.
Pure PPy	PPy microspheres	10 mm	−12 dB	15	5–20 mm	6 GHz	75
	PPy nanorods	3.1 mm	−45 dB	15	2.2 mm	5.6 GHz	76
	3D PPy aerogel	2.0 mm	−35 dB	7	2.5 mm	6.2 GHz	77
	LHF-PPy nanofibers	2.4 mm	−41 dB	7	2.4 mm	7.4 GHz	78
Binary PPy	$ZnFe_2O_4$/PPy	—	−28.9 dB	50	—	4.2 GHz	79
	Fe_3O_4/PPy	2.3 mm	−22.4 dB	50	2.3 mm	5.0 GHz	80
	PPy/$ZCCFS_{0.04}$O. (20 wt%)	2.0 mm	−20.9 dB	50	2.0 mm	11.3 GHz	81
	Ni/PPy (4:1)	2.0 mm	−15.2 dB	50	2.0 mm	4.4 GHz	82
	Co/PPy	2.0 mm	−33 dB	30	2.0 mm	4.77 GHz	83
	SnO_2/PPy aerogel	3.0 mm	−46.14 dB	7	3.0 mm	7.28 GHz	84
	Carbonyl Iron/PPy (20:1)	—	−16 dB	60	—	1.8 GHz	85
	PPy/exfoliated Graphite1.5	2.5 mm	−34 dB	10	2–5 mm	13 GHz	86
	PPy@PANI-1.2	2.0 mm	−34.8 dB	50	2.0 mm	4.7 GHz	87
PPy Composite	Multi-Fe_3O_4/PPy/CNT	3.0 mm	−25.9 dB	20	3.0 mm	4.5 GHz	88
	PPy/FeCo/SiO_2	2.1 mm	−65.17 dB	33	2.1–5 mm	6.8 GHz	89
	Graphene/PPy/Fe_3O_4	5.3 mm	−56.9 dB	—	3–7 mm	15.1 GHz	90
	PPy/$NiFe_2O_4$/rGO	1.7 mm	−44.8 dB	50	1.7 mm	5.3 GHz	91
	rGO/CuS/PPy	4.0 mm	−49.11 dB	10	2.0 mm	4.88 GHz	92
	PPy/NR/Fe_3O_4	2.0 mm	−32 dB	—	2.0 mm	9.0 GHz	93

the conductive properties of various polymer nanocomposites. After percolation, the DC conductivity of nanomaterials may exhibit an extremely high degree of conductivity. The electrical conductivity of polymeric nanomaterials obeys a power relationship called the law of proportionality due to the presence of conductive nanoparticles.[97] This relationship is expressed as follows:

$$\sigma_{dc}\,(p) = \sigma_0\,(p - p^c)^t \qquad (7)$$

where p and p^c represent the concentration ratio of the nanofiller and percolation threshold, respectively, while t represents the perilous exponent that varies with the structural dimensions. For 2d systems, the value of t is 1.3 but in 3d networks it varies between 1.6 and 2. Studies have revealed that electrical improvements to the conductivity can be made due to the creation of an arrangement of conductive nanofillers inside a polymer matrix. Using a highly significant proportion of conductive particles, the percolation threshold can be reduced. From previous literature, it is clear that EM attenuation can be optimized by generating a series of nanoparticles. It has also been shown that different strategies, such as covalent and non-covalent coupling with polymer chain functionalization, can improve the dispersion of nanoparticles. Dielectric properties, such as real, imaginary, and complex permittivity, play an important role in absorbing electromagnetic waves. A high value of dielectric constant, together with dielectric loss, can improve radiation absorption in the microwave zone.[98] A block diagram of an EMI-SE measurement vector network analyzer scheme is shown in Fig. 12.

4.3 Microwave electromagnetic absorption properties

The microwave absorption properties of materials in terms of loss due to reflection or return loss R_L in dB can be expressed by the following equation:

$$R_L = 20\log|Z_{in} - Z_o|/|Z_{in} + Z_o| \qquad (8)$$

where Z_{in} is the input impedance of the shield and Z_o is the free space impedance (Z_o = 377 Ω).

Maximum absorption occurs when the minimum reflection loss ($R_{L_{min}}$) is reached, which means that the input impedance of the absorber and free space impedance are matched. It has been reported that shielding materials with an R_L at the level of 10 dB can absorb 90% of the incident electromagnetic radiation, which is considered sufficiently effective for most common applications. Materials with a shielding performance equivalent to 20 dB are capable of absorbing 99% of incident electromagnetic radiation. Therefore, the prepared composites must provide a reflection attenuation of at least 10 dB or less to be effective EMI absorbers.[41]

A high electrical conductivity of conductive materials seems to be the only key factor for its shielding effectiveness due to the high tan dE (> 1). On the other hand, in materials with poor electrical conductivity (tan dE $\ll$ 1), the permittivity and conductivity are both important properties of inherently conductive polymers and polymer composites. Therefore, modification of the electromagnetic characteristics and thickness of
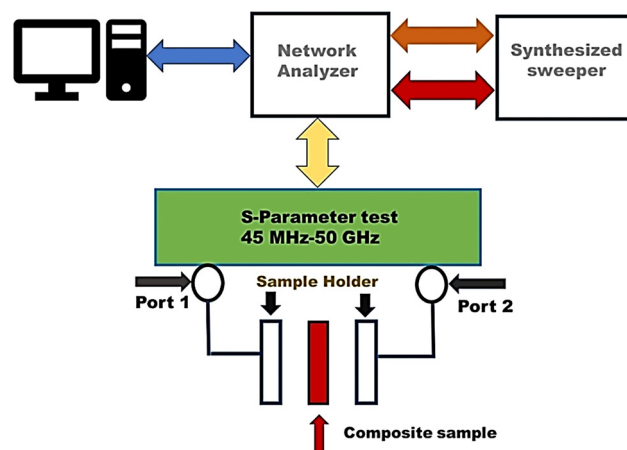

Fig. 12 Block diagram of an EMI-SE measurement vector network analyzer scheme.

the EMI shield are important to obtain adequate shielding and establish the appropriate shielding mechanism.[99,100]

There are also other requirements for effective EMI shields, such as light weight, corrosive and chemical properties resistance, minimal thickness, good elasticity and flexibility, applicable mechanical properties, easily fabrication, and an acceptable price.

5. Conclusion and future perspective

Polypyrroles as a significant class of conductive polymers have demonstrated promising potential as an electromagnetic absorbing material. This review began by providing an overview of the background, definition, absorption parameters, and mechanisms of electromagnetic absorbing materials. Subsequently, it delved into recent advancements and absorption mechanisms related to materials based on PPy for electromagnetic absorption. Some of the key points are summarized below.

● Barium strontium titanate (BST), reduced graphene oxide (RGO), and Fe_3O_4 [BRF] nanoparticles were synthesized through a chemical oxidative polymerization process of pyrrole. The addition of these filler materials into the conducting polymer matrix led to a significant improvement in its shielding effectiveness, particularly in the X-band frequency range of 8.2–12.4 GHz. This absorption-dominated shielding effectiveness value reached an impressive 48 dB when Fe_3O_4 nanoparticles were incorporated in the composites, endowing them with the advantages of high magnetization, small size, corrosion resistance, environmental friendliness, and economical.

● α-Fe_2O_3/PPy/CDCA (referred to as FPCA) exhibited the highest overall shielding effectiveness (SE_{total}) at 39.4 dB. The remarkably increasing trends reflected that the existence of α-Fe_2O_3 and PPy could effectively facilitate the improvement of the EMI shielding property of composites. Notably, the shielding effectiveness attributed to absorption accounted for a significant portion (ranging from 78.2–84.2%) of the SE_{total}

for FPCA, indicating that an absorption-dominant shielding mechanism played a crucial role in mitigating secondary radiation. The SE_{total} value of FCPA was comparable to or even slightly higher than that of previously reported carbon-based EMI shields, such as exfoliated few layer graphene (12 dB), carbon fiber/silica (12.4 dB), and biomorphic porous carbon (40 dB).

• The favorable conductivity of PPy plays a crucial role in enhancing conduction losses and absorbing electromagnetic waves with metal oxides; whereby the integration of PPy with these inorganic additives typically generates noticeable synergetic effects and complementary behaviors. This integration introduces additional loss mechanisms, significantly contributing to the overall microwave absorption performance.

• This review underscores the critical importance of the interfaces between embedded fillers and polymers, highlighting their potential for effective optimization across a spectrum of frequency bands. Such optimized composites hold significant promise for a wide array of applications across industrial, military, consumer, and medical sectors, encompassing diverse electro/electrical systems.

While notable progress has been made in the development of PPy absorbing materials, several challenges persist, primarily evident in the following areas:

• The interaction within the composite systems is not merely additive. Further exploration is required to understand the impact of the interactions between the components on the absorbing properties.

• Polypyrrole (PPy) inherently contains nitrogen atoms, and during the polymerization process using an oxidant, it becomes doped with ions. The impact of these dopants on the electromagnetic absorption properties of PPy requires further investigation. Additionally, the interaction between PPy and other materials in PPy-based composites remains unclear. Contemporary advancements in characterization testing techniques, such as X-ray absorption spectroscopy (XAS), scanning transmission electron microscopy (STEM), and various *in situ* methods, provide opportunities for a more in-depth exploration of the correlation between the material's interior and its electromagnetic absorbing properties.

• The electromagnetic properties of conducting polymer composites are significantly influenced by the size, shape, and concentration of fillers. Despite considerable exploration and analysis, effective solutions for achieving robust tunability in electromagnetic interference (EMI) shielding properties are still lacking.

• Very few reports are available on the EMI shielding of PPy with metal sulfides, which could be further used for future studies.

Conflicts of interest

On behalf of all authors, each corresponding author states that they have no conflicts of interest to declare.

References

1 X. Liang, B. Quan, Z. Man, B. Cao, N. Li, C. Wang, G. Ji and T. Yu, *ACS Appl. Mater. Interfaces*, 2019, **11**, 30228–30233.

2 H. Lv, Z. Yang, P. L. Wang, G. Ji, J. Song, L. Zheng, H. Zeng and Z. J. Xu, *Adv. Mater.*, 2018, **30**, 1706343.

3 Z. Wu, K. Pei, L. Xing, X. Yu, W. You and R. Che, *Adv. Funct. Mater.*, 2019, **29**, 1901448.

4 J. Chang, H. Zhai, Z. Hu and J. Li, *Composites, Part B*, 2022, **246**, 110269.

5 S. Sadki, P. Schottland, N. Brodie and G. Sabouraud, *Chem. Soc. Rev.*, 2000, **29**, 283–293.

6 J. Janata and M. Josowicz, *Nat. Mater.*, 2003, **2**, 19–24.

7 A. Joshi and S. Datar, *Pramana*, 2015, **84**, 1099–1116.

8 L. Geng, P. Zhu, Y. Wei, R. Guo, C. Xiang, C. Cui and Y. Li, *Cellulose*, 2019, **26**, 2833–2847.

9 B. Zhang, J. Wang, J. Wang, H. Duan, S. Huo and Y. Tang, *J. Mater. Sci.: Mater. Electron.*, 2017, **28**, 3337–3348.

10 R. Kanwal, M. F. Maqsood, M. A. Raza, A. Inam, M. Waris, Z. U. Rehman, S. M. Z. Mehdi, N. Abbas and N. Lee, *Mater. Today Commun.*, 2024, **38**, 107684.

11 M. F. Shakir, I. Abdul Rashid, A. Tariq, Y. Nawab, A. Afzal, M. Nabeel, A. Naseem and U. Hamid, *J. Electron. Mater.*, 2020, **49**, 1660–1665.

12 T. Su, B. Zhao, F. Han, B. Fan and R. Zhang, *J. Mater. Sci.: Mater. Electron.*, 2019, **30**, 475–484.

13 M. K. Vyas and A. Chandra, *J. Mater. Sci.*, 2019, **54**, 1304–1325.

14 S. Li, C. Yang, S. Sarwar, A. Nautiyal, P. Zhang, H. Du, N. Liu, J. Yin, K. Deng and X. Zhang, *Adv. Compos. Hybrid Mater.*, 2019, **2**, 279–288.

15 L. Yuan, W. Zhao, Y. Miao, C. Wang, A. Cui, Z. Tian, T. Wang, A. Meng, M. Zhang and Z. Li, *Adv. Compos. Hybrid Mater.*, 2024, **7**, DOI: **10.1007/s42114-024-00864-z**.

16 D. D. L. Chung, *Composites, Part B*, 2019, **160**, 644–660.

17 A. Rayar, C. S. Naveen, H. S. Onkarappa, V. S. Betageri and G. D. Prasanna, *Synth. Met.*, 2023, **295**, 117338.

18 Y. Sood, S. D. Lawaniya, H. Mudila, K. Awasthi and A. Kumar, *Sens. Actuators, B*, 2023, **394**, 134298.

19 L. Ma, L. Wei, M. Hamidinejad and C. B. Park, *Mater. Horiz.*, 2023, **10**, 4423–4437.

20 Y. Sood, H. Mudila, A. Katoch, P. E. Lokhande, D. Kumar, A. Sharma and A. Kumar, *J. Mater. Sci.: Mater. Electron.*, 2023, **34**(18), 1401.

21 J. Azadmanjiri, P. Hojati-Talemi, G. P. Simon, K. Suzuki and C. Selomulya, *Polym. Eng. Sci.*, 2011, **51**, 247–253.

22 Y. Sood, A. Kumar and H. Mudila, *J. Phys.: Conf. Ser.*, 2022, **2267**, 012050.

23 Y. Sood, V. S. Pawar, H. Mudila and A. Kumar, *Polym. Eng. Sci.*, 2021, **61**, 2949–2973.

24 A. Pandey, R. Kumar, D. P. Mondal, P. Kumar and S. Singh, *Mater. Today Nano*, 2023, **21**, 100301.

25 Y. Yang, M. C. Gupta, K. L. Dudley and R. W. Lawrence, *Nano Lett.*, 2005, **5**, 2131–2134.

26 A. Kaur and S. K. Dhawan, *Synth. Met.*, 2012, **162**, 1471–1477.

27 J. D. Sudha, S. Sivakala, K. Patel and P. Radhakrishnan Nair, *Composites, Part A*, 2010, **41**, 1647–1652.

28 F. J. López-Rodríguez and G. G. Naumis, *Phys. Rev. B: Condens. Matter Mater. Phys.*, 2009, **79**, 049901.

29 M. Cao, C. Han, X. Wang, M. Zhang, Y. Zhang, J. Shu, H. Yang, X. Fang and J. Yuan, *J. Mater. Chem. C*, 2018, **6**, 4586–4602.

30 T. Zhao, C. Hou, H. Zhang, R. Zhu, S. She, J. Wang, T. Li, Z. Liu and B. Wei, *Sci. Rep.*, 2014, **4**, 5617.

31 L. Wei and Y. N. Wang, *Phys. Lett. Sect. A Gen. At. Solid State Phys*, 2004, **333**, 303–309.

32 M. Oyharçabal, T. Olinga, M. P. Foulc, S. Lacomme, E. Gontier and V. Vigneras, *Compos. Sci. Technol.*, 2013, **74**, 107–112.

33 H. Yu, T. Wang, B. Wen, M. Lu, Z. Xu, C. Zhu, Y. Chen, X. Xue, C. Sun and M. Cao, *J. Mater. Chem.*, 2012, **22**, 21679–21685.

34 S. J. Yan, L. Zhen, C. Y. Xu, J. T. Jiang, W. Z. Shao and J. K. Tang, *J. Magn. Magn. Mater.*, 2011, **323**, 515–520.

35 Y. Naito and K. Suetake, *IEEE Trans. Microw. Theory Tech.*, 1971, **19**, 65–72.

36 R. Kumar, S. Sahoo, E. Joanni and J. J. Shim, *Composites, Part B*, 2023, **264**, 110874.

37 T. A. Jones, J. G. Firth and B. Mann, *Sens. Actuators*, 1985, **8**, 281–306.

38 Y. Zhang, J. Ning, L. Hou, J. Kidd, M. Foley, J. Zhang, R. Jin, J. Sun and W. Plummer, *J. Phys. Chem. Solids*, 2021, **150**, 109803.

39 J. Luo and D. Gao, *J. Magn. Magn. Mater.*, 2014, **368**, 82–86.

40 A. Olad and S. Shakoori, *J. Magn. Magn. Mater.*, 2018, **458**, 335–345.

41 V. Shukla, *Nanoscale Adv.*, 2019, **1**, 1640–1671.

42 F. Du, J. E. Fischer and K. I. Winey, *Phys. Rev. B: Condens. Matter Mater. Phys.*, 2005, **72**, 121404.

43 S. Dutta and S. K. Pati, *J. Mater. Chem.*, 2010, **20**, 8207–8223.

44 D. Kumar, A. Moharana and A. Kumar, *Mater. Today Chem.*, 2020, **17**, 100346.

45 S. Geetha, K. K. S. Kumar, C. R. K. Rao, M. Vijayan and D. C. Trivedi, *J. Appl. Polym. Sci.*, 2009, **112**, 2073–2086.

46 I. Ebrahimi and M. P. Gashti, *J. Phys. Chem. Solids*, 2018, **118**, 80–87.

47 A. Pasha, S. Khasim, A. A. A. Darwish, T. A. Hamdalla, S. A. Al-Ghamdi and S. Alfadhli, *Synth. Met.*, 2022, **283**, 116984.

48 X. Li, H. Yi, J. Zhang, J. Feng, F. Li, D. Xue, H. Zhang, Y. Peng and N. J. Mellors, *J. Nanoparticle Res.*, 2013, **15**, DOI: 10.1007/s11051-013-1472-1.

49 P. Sambyal, S. K. Dhawan, P. Gairola, S. S. Chauhan and S. P. Gairola, *Curr. Appl. Phys.*, 2018, **18**, 611–618.

50 C. H. A. Kadar, M. Faisal, N. Raghavendra, N. Maruthi, B. P. Prasanna and K. R. Nandan, *J. Mater. Sci.: Mater. Electron.*, 2022, **33**, 14188–14201.

51 U. Anwar, N. Sultan, G. Yasmeen, K. Shati and M. Nadeem, *Heliyon*, 2023, **9**, e23193.

52 V. Q. Trung, D. N. Tung and D. N. Huyen, *J. Exp. Nanosci.*, 2009, **4**, 213–219.

53 X. Yang, K. Fu, L. Wu, X. Tang, J. Wang, G. Tong, D. Chen and W. Wu, *Carbon N. Y.*, 2022, **199**, 1–12.

54 C. Wan and J. Li, *Carbohydr. Polym.*, 2017, **161**, 158–165.

55 W. L. Song, M. S. Cao, M. M. Lu, J. Yang, H. F. Ju, Z. L. Hou, J. Liu, J. Yuan and L. Z. Fan, *Nanotechnology*, 2013, **24**, 115708.

56 M. S. Cao, W. L. Song, Z. L. Hou, B. Wen and J. Yuan, *Carbon N. Y.*, 2010, **48**, 788–796.

57 X. Liu, X. Yin, L. Kong, Q. Li, Y. Liu, W. Duan, L. Zhang and L. Cheng, *Carbon N. Y.*, 2014, **68**, 501–510.

58 B. M. Basavaraja Patel, M. Revanasiddappa, S. Yallappa and D. R. Rangaswamy, *J. Mater. Sci.: Mater. Electron.*, 2023, **34**, 866.

59 B. M. B. Patel, M. Revanasiddappa, D. R. Rangaswamy, S. Manjunatha and Y. T. Ravikiran, *Mater. Today Proc.*, 2021, **49**, 2253–2259.

60 S. Ganguly, N. Kanovsky, P. Das, A. Gedanken and S. Margel, *Adv. Mater. Interfaces*, 2021, **8**, 2102155.

61 S. Varshney, K. Singh, A. Ohlan, V. K. Jain, V. P. Dutta and S. K. Dhawan, *J. Alloys Compd.*, 2012, **538**, 107–114.

62 I. Ahmad, M. Zeshan, M. M. Alanazi, S. A. M. Abdelmohsen and H. M. T. Farid, *Curr. Appl. Phys.*, 2023, **51**, 64–70.

63 L. K. Dhugga, H. B. Baskey, K. K. Gaur and D. P. Singh, *Compos. Sci. Technol.*, 2023, **240**, 110067.

64 C. Liu and X. Liao, *ACS Appl. Nano Mater.*, 2020, **3**, 11906–11915.

65 S. Varshney, A. Ohlan, V. K. Jain, V. P. Dutta and S. K. Dhawan, *Ind. Eng. Chem. Res.*, 2014, **53**, 14282–14290.

66 K. Benzaoui, A. Ales, A. Mekki, A. Zaoui, B. Bouaouina, A. Singh, O. Mehelli and M. Derradji, *High Perform. Polym.*, 2022, **34**, 310–320.

67 H. Zhao, L. Hou and Y. Lu, *Chem. Eng. J.*, 2016, **297**, 170–179.

68 B. M. B. Patel, M. Revanasiddappa and D. R. Rangaswamy, *J. Electron. Mater.*, 2022, **51**, 6937–6950.

69 T. Lin, H. Yu, Y. Wang, L. Wang, S. Z. Vatsadze, X. Liu, Z. Huang, S. Ren, M. A. Uddin, B. U. Amin and S. Fahad, *J. Mater. Sci.*, 2021, **56**, 18093–18115.

70 H. M. Rashmi, M. Revanasiddappa, B. N. Ramakrishna, M. Surekha, D. R. Rangaswamy and S. Yallappa, *Polym. Sci., Ser. B*, 2023, **65**, 963–973.

71 J. Srivastava, P. Kumar Khanna, P. V. More and N. Singh, *Adv. Mater. Lett.*, 2017, **8**, 42–48.

72 K. Sun, X. Yang, Y. Lei, H. Du, T. Dudziak and R. Fan, *J. Alloys Compd.*, 2023, **930**, 167446.

73 C. Xing, Y. Hao, A. Xia, G. Guo, L. Dong, J. Xu, Y. Kang and W. Huang, *Synth. Met.*, 2024, **306**, 117628.

74 V. Shukla, *J. Mater. Sci.*, 2020, **55**, 2826–2835.

75 H. Farrokhi, O. Khani, F. Nemati and M. Jazirehpour, *Synth. Met.*, 2016, **215**, 142–149.

76 O. Khani, F. Nemati, H. Farrokhi and M. Jazirehpour, *Synth. Met.*, 2016, **220**, 567–572.

77 A. Xie, F. Wu, M. Sun, X. Dai, Z. Xu, Y. Qiu, Y. Wang and M. Wang, *Appl. Phys. Lett.*, 2015, **106**, 222902.

78 A. Xie, F. Wu, W. Jiang, K. Zhang, M. Sun and M. Wang, *J. Mater. Chem. C*, 2017, **5**, 2175–2181.

79 Y. Li, R. Yi, A. Yan, L. Deng, K. Zhou and X. Liu, *Solid State Sci.*, 2009, **11**, 1319–1324.

80 Y. Li, G. Chen, Q. Li, G. Qiu and X. Liu, *J. Alloys Compd.*, 2011, **509**, 4104–4107.

81 Y. Wang, Y. Huang, Q. Wang, Q. He and L. Chen, *Appl. Surf. Sci.*, 2012, **259**, 486–493.

82 P. Xu, X. Han, C. Wang, D. Zhou, Z. Lv, A. Wen, X. Wang and B. Zhang, *J. Phys. Chem. B*, 2008, **112**, 10443–10448.

83 H. Wang, N. Ma, Z. Yan, L. Deng, J. He, Y. Hou, Y. Jiang and G. Yu, *Nanoscale*, 2015, **7**, 7189–7196.

84 Y. Wang, X. Dai, W. Jiang, F. Wu and A. Xie, *Mater. Res. Express*, 2016, **3**, 075023.

85 D. A. Li, H. Bin Wang, J. M. Zhao and X. Yang, *Mater. Chem. Phys.*, 2011, **130**, 437–441.

86 L. Shan, X. Chen, X. Tian, J. Chen, Z. Zhou, M. Jiang, X. Xu and D. Hui, *Composites, Part B*, 2015, **73**, 181–187.

87 C. Tian, Y. Du, P. Xu, R. Qiang, Y. Wang, D. Ding, J. Xue, J. Ma, H. Zhao and X. Han, *ACS Appl. Mater. Interfaces*, 2015, **7**, 20090–20099.

88 R. Bin Yang, P. M. Reddy, C. J. Chang, P. A. Chen, J. K. Chen and C. C. Chang, *Chem. Eng. J.*, 2016, **285**, 497–507.

89 S. Li, Y. Huang, N. Zhang, M. Zong and P. Liu, *J. Alloys Compd.*, 2019, **774**, 532–539.

90 P. Liu, Y. Huang and X. Zhang, *Mater. Lett.*, 2014, **129**, 35–38.

91 J. Yan, Y. Huang, X. Chen and C. Wei, *Synth. Met.*, 2016, **221**, 291–298.

92 B. Zhang, S. Lin, J. Zhang, X. Li and X. Sun, *Materials*, 2020, **13**, 446.

93 N. Rezazadeh, A. Kianvash and P. Palmeh, *J. Appl. Polym. Sci.*, 2018, **135**, 46565.

94 B. Zhao, G. Shao, B. Fan, W. Zhao and R. Zhang, *Phys. Chem. Chem. Phys.*, 2015, **17**, 2531–2539.

95 S. Yamada and E. Otsuki, *J. Appl. Phys.*, 1997, **81**, 4791–4793.

96 P. Liu, S. Gao, Y. Wang, Y. Huang, F. Zhou and P. Liu, *Carbon N. Y.*, 2021, **173**, 655–666.

97 S. Siddique, M. Zahid, R. Anum, H. F. Shakir and Z. A. Rehan, *Results Phys.*, 2021, **24**, 104183.

98 A. Celzard, E. McRae, C. Deleuze and M. Dufort, *Phys. Rev. B: Condens. Matter Mater. Phys.*, 1996, **53**, 6209–6214.

99 Z. Wang, R. Wei, J. Gu, H. Liu, C. Liu, C. Luo, J. Kong, Q. Shao, N. Wang, Z. Guo and X. Liu, *Carbon N. Y.*, 2018, **139**, 1126–1135.

100 Z. W. Li and Z. H. Yang, *J. Magn. Magn. Mater.*, 2015, **391**, 172–178.